

Self-Distillation Amplifies Regularization in Hilbert Space

Hossein Mobahi* Mehrdad Farajtabar[§] Peter L. Bartlett*[†]

hmobahi@google.com farajtabar@google.com bartlett@eecs.berkeley.edu

*Google Research, Mountain View, CA, USA

[§] DeepMind, Mountain View, CA, USA

[†]EECS Dept., University of California at Berkeley, Berkeley, CA, USA

Abstract

Knowledge distillation introduced in the deep learning context is a method to transfer knowledge from one architecture to another. In particular, when the architectures are identical, this is called self-distillation. The idea is to feed in predictions of the trained model as new target values for retraining (and iterate this loop possibly a few times). It has been empirically observed that the self-distilled model often achieves higher accuracy on held out data. Why this happens, however, has been a mystery: the self-distillation dynamics does not receive any new information about the task and solely evolves by looping over training. To the best of our knowledge, there is no rigorous understanding of why this happens. This work provides the first theoretical analysis of self-distillation. We focus on fitting a nonlinear function to training data, where the model space is Hilbert space and fitting is subject to ℓ_2 regularization in this function space. We show that self-distillation iterations modify regularization by progressively limiting the number of basis functions that can be used to represent the solution. This implies (as we also verify empirically) that while a few rounds of self-distillation may reduce over-fitting, further rounds may lead to under-fitting and thus worse performance.

1 Introduction

Knowledge distillation, originally introduced in the deep learning setting [Hinton et al., 2015], is a method that transfers knowledge from one architecture (teacher) to another (student), where often the student model is much smaller. The original formulation achieves this by training the student model using the output probability distribution of the teacher model in addition to original labels. The student model benefits from this “dark knowledge” (extra information in soft predictions) and often performs better than if it was trained on the actual labels.

Various extensions of this approach have been recently proposed, where instead of output predictions, the student matches other statistics from the teacher model such as intermediate feature representations [Romero et al., 2014], Jacobian matrices [Srinivas and Fleuret, 2018], distributions [Huang and Wang, 2017], Gram matrices [Yim et al., 2017]. Additional developments on knowledge distillation include its extensions to Bayesian settings [Korattikara Balan et al., 2015, Vadera and Marlin, 2020], uncertainty preservation [Tran et al., 2020], reinforcement learning [Hong et al., 2020, Teh et al., 2017, Ghosh et al., 2018], online distillation [lan et al., 2018], zero-shot learning [Nayak et al., 2019], multi-step knowledge distillation [Mirzadeh et al., 2020], tackling catastrophic forgetting [Li and Hoiem, 2016], transfer of relational knowledge [Park et al., 2019], adversarial distillation [Wang et al., 2018].

The special case when the teacher and student architectures are identical is called¹ *self-distillation*. The idea is to feed in predictions of the trained model as new target values for retraining (and iterate this loop possibly a few times). It has been consistently observed that the self-distilled model often achieves higher accuracy on held out data [Furlanello et al., 2018, Yang et al., 2019, Ahn et al., 2019]. Why this happens, however, has been a mystery: the self-distillation dynamics does not receive any new information about the task and solely evolves by looping over training. There have been some recent attempts to understand the mysteries around distillation. [Gotmare et al., 2019] have empirically observed that the dark knowledge transferred by the teacher is localized mainly in higher layers and does not affect early (feature extraction) layers much. [Furlanello et al., 2018] interprets dark knowledge as importance weighting. [Dong et al., 2019] shows that early-stopping is crucial for reaching dark-knowledge of self-distillation.

Despite these interesting developments, why distillation can improve generalization remains illusive. To the best of our knowledge, there is no rigorous understanding of why this happens. This work provides a *theoretical analysis of self-distillation*. We focus on fitting a nonlinear function to training data, where the models belong to a Hilbert space and fitting is subject to ℓ_2 regularization in this function space. We show that self-distillation iterations modify regularization by progressively limiting the number of basis functions that can be used to represent the solution. This implies (as we also verify empirically) that while a few rounds of self-distillation may reduce over-fitting, further rounds may lead to under-fitting and thus worse performance.

This paper is organized as follows. In Section 2 we setup a variational formulation for nonlinear regression and discuss the existence of non-trivial solutions for it. Section 3 formalizes self-distillation in our setting and shows that self-distillation iterations cannot continue indefinitely; at some point the solution collapses. It then provides a lower bound on the number of distillation iterations before the solution collapses. In addition, it shows that the basis functions initially used to represent the solution gradually change to a more sparse representation. Finally, we discuss the advantage of models operating in the near-interpolation regime; this ultimately achieves a higher sparsity level. Section 5 draws connection between our setting and the NTK regime of neural networks. This motivates subsequent experiments on deep neural networks in that section.

To facilitate the presentation of analyses in Sections 2 and 3, we present our results in small steps as propositions. Full proofs for these propositions are provided in the supplementary appendix. In addition, codes to generate the illustrative example of Sections 4 and 5 are available in the appendix.

2 Problem Setup

We first introduce some notation. We denote a set by \mathcal{A} , a matrix by \mathbf{A} , a vector by \mathbf{a} , and a scalar by a or A . The (i, j) 'th component of a matrix is denoted by $\mathbf{A}[i, j]$ and the i 'th component of a vector by $\mathbf{a}[i]$. Also $\|\cdot\|$ refers to ℓ_2 norm of a vector. We use \triangleq to indicate equal by definition. A linear operator L applied to a function f is shown by $[Lf]$, and when evaluated at point x by $[Lf](x)$. For a positive definite matrix \mathbf{A} , we use κ to refer to its condition number $\kappa \triangleq \frac{d_{\max}}{d_{\min}}$, where d 's are eigenvalues of \mathbf{A} .

Consider a finite training set $\mathcal{D} \triangleq \cup_{k=1}^K \{(\mathbf{x}_k, y_k)\}$, where $\mathbf{x}_k \in \mathcal{X} \subseteq \mathbb{R}^d$ and $y_k \in \mathcal{Y} \subseteq \mathbb{R}$. Consider a space of all admissible functions (as we define later in this section) $\mathcal{F} : \mathcal{X} \rightarrow \mathcal{Y}$. The goal is to use this training data to find a function $f^* : \mathcal{X} \rightarrow \mathcal{Y}$ that approximates the underlying mapping from \mathcal{X} to \mathcal{Y} . We assume the function space \mathcal{F} is rich enough to contain multiple functions that can fit finite training data. Thus, the presence of an adequate inductive bias is essential to guide the training process towards solutions that generalize. We infuse such bias in training via regularization. Specifically, we

¹The term self-distillation has been used to describe a variety of related ideas in recent literature. We adopt the formulation described in [Furlanello et al., 2018], which is explained in our Section 3. This concept is a supervised counterpart of self-training in unsupervised and semisupervised learning.

study regression problems of form²,

$$f^* \triangleq \arg \min_{f \in \mathcal{F}} R(f) \quad \text{s.t.} \quad \frac{1}{K} \sum_k (f(\mathbf{x}_k) - y_k)^2 \leq \epsilon, \quad (1)$$

where $R : \mathcal{F} \rightarrow \mathbb{R}$ is a regularization functional, and $\epsilon > 0$ is a desired loss tolerance. We study regularizers with the following form,

$$R(f) = \int_{\mathcal{X}} \int_{\mathcal{X}} u(\mathbf{x}, \mathbf{x}^\dagger) f(\mathbf{x}) f(\mathbf{x}^\dagger) d\mathbf{x} d\mathbf{x}^\dagger, \quad (2)$$

with u being such that $\forall f \in \mathcal{F}; R(f) \geq 0$ with *equality* only when $f(\mathbf{x}) = 0$. Without loss of generality³, we assume u is symmetric $u(\mathbf{x}, \mathbf{x}^\dagger) = u(\mathbf{x}^\dagger, \mathbf{x})$. For a given u , the space \mathcal{F} of admissible functions are f 's for which the double integral in (2) is bounded.

The conditions we imposed on $R(f)$ implies that the operator L defined as $[Lf] \triangleq \int_{\mathcal{X}} u(\mathbf{x}, \cdot) f(\mathbf{x}) d\mathbf{x}$ has an empty null space⁴. The symmetry and non-negativity conditions together are called **Mercer's condition** and u is called a kernel. Constructing R via kernel u can cover a wide range of regularization forms including⁵,

$$R(f) = \int_{\mathcal{X}} \sum_{j=1}^J w_j ([P_j f](\mathbf{x}))^2 d\mathbf{x}, \quad (3)$$

where P_j is some linear operator (e.g. a differential operator to penalize non-smooth functions as we will see in Section 4), and $w_j \geq 0$ is some weight, for $j = 1, \dots, J$ operators.

Plugging $R(f)$ into the objective functional leads to the following variational problem,

$$\begin{aligned} f^* \triangleq \arg \min_{f \in \mathcal{F}} & \int_{\mathcal{X}} \int_{\mathcal{X}} u(\mathbf{x}, \mathbf{x}^\dagger) f(\mathbf{x}) f(\mathbf{x}^\dagger) d\mathbf{x} d\mathbf{x}^\dagger \\ & \text{s.t.} \quad \frac{1}{K} \sum_k (f(\mathbf{x}_k) - y_k)^2 \leq \epsilon. \end{aligned} \quad (4)$$

The Karush-Kuhn-Tucker (KKT) condition for this problem yields,

$$f_\lambda^* \triangleq \arg \min_{f \in \mathcal{F}} \frac{\lambda}{K} \sum_k (f(\mathbf{x}_k) - y_k)^2 \quad (5)$$

$$+ \int_{\mathcal{X}} \int_{\mathcal{X}} u(\mathbf{x}, \mathbf{x}^\dagger) f(\mathbf{x}) f(\mathbf{x}^\dagger) d\mathbf{x} d\mathbf{x}^\dagger \quad (6)$$

$$\text{s.t.} \quad \lambda \geq 0 \quad , \quad \frac{1}{K} \sum_k (f(\mathbf{x}_k) - y_k)^2 \leq \epsilon \quad (7)$$

$$\lambda \left(\frac{1}{K} \sum_k (f(\mathbf{x}_k) - y_k)^2 - \epsilon \right) = 0. \quad (8)$$

²Our choice of setting up learning as a constrained optimization rather than unconstrained form $\frac{1}{K} \sum_k (f(\mathbf{x}_k) - y_k)^2 + cR(f)$ is motivated by the fact that we often have control over ϵ as a user-specified stopping criterion. In fact, in the era of overparameterized models, we can often fit training data to a desired ϵ -optimal loss value [Zhang et al., 2016]. However, if we adopt the unconstrained setting, it is unclear what value of c would correspond to a particular stopping criterion.

³If u is not symmetric, we define a new function $u^\diamond \triangleq \frac{1}{2}(u(\mathbf{x}, \mathbf{x}^\dagger) + u(\mathbf{x}^\dagger, \mathbf{x}))$ and work with that instead. Note that u^\diamond is symmetric and satisfies $R_u(f) = R_{u^\diamond}(f)$.

⁴This is a technical assumption for simplifying the exposition. If the null space is non-empty, one can still utilize it using [Girosi et al., 1995].

⁵To see that, let's rewrite $\int_{\mathcal{X}} \sum_j w_j (P_j f(\mathbf{x}))^2 d\mathbf{x}$ by a more compact form $\sum_j w_j \langle P_j f, P_j f \rangle$. Observe that $\sum_j w_j \langle P_j f, P_j f \rangle = \sum_j w_j \langle f, P_j^* P_j f \rangle = \langle f, (\sum_j w_j P_j^* P_j) f \rangle = \langle f, U f \rangle$, where P_j^* denotes the adjoint operator of P_j , and $U \triangleq \sum_j w_j P_j^* P_j$. Notice that $P_j^* P_j$ is a positive definite operator. Scaling it by the non-negative scalar w_j still keeps the resulted operator positive definite. Finally, a sum of positive-definite operators is positive definite. Thus U is a positive definite operator. Switching back to the integral notation, this gives exactly the requirement we had on choosing u ,

$$\forall f \in \mathcal{F}; \int_{\mathcal{X}} u(\mathbf{x}, \mathbf{x}^\dagger) f(\mathbf{x}) f(\mathbf{x}^\dagger) d\mathbf{x} d\mathbf{x}^\dagger \geq 0.$$

2.1 Existence of Non-Trivial Solutions

Stack training labels into a vector,

$$\mathbf{y}_{K \times 1} \triangleq [y_1 | y_2 | \dots | y_K]. \quad (9)$$

It is obvious that when $\frac{1}{K}\|\mathbf{y}\|^2 \leq \epsilon$, then f^* has trivial solution $f^*(\mathbf{x}) = 0$, which we refer to this case as *collapse* mode. In the sequel, we focus on the more interesting case of $\frac{1}{K}\|\mathbf{y}\|^2 > \epsilon$. It is also easy to verify that collapsed solution is tied to $\lambda = 0$,

$$\|\mathbf{y}\|^2 > K\epsilon \Leftrightarrow \lambda > 0. \quad (10)$$

Thus by taking any $\lambda > 0$ that satisfies $\frac{1}{K}\sum_k (f_\lambda^*(\mathbf{x}_k) - y_k)^2 - \epsilon = 0$, the following form f_λ^* is an optimal solution to the problem (4), i.e. $f^* = f_\lambda^*$.

$$f_\lambda^* = \arg \min_{f \in \mathcal{F}} \frac{\lambda}{K} \sum_k (f(\mathbf{x}_k) - y_k)^2 \quad (11)$$

$$+ \int_{\mathcal{X}} \int_{\mathcal{X}} u(\mathbf{x}, \mathbf{x}^\dagger) f(\mathbf{x}) f(\mathbf{x}^\dagger) d\mathbf{x} d\mathbf{x}^\dagger. \quad (12)$$

2.2 Closed Form of f^*

In this section we present a closed form expression for (11). Since we are considering $\lambda > 0$, without loss of generality, we can divide the objective function in (11) by λ and let $c \triangleq 1/\lambda$; obviously $c > 0$.

$$f^* = \arg \min_{f \in \mathcal{F}} \frac{1}{K} \sum_k (f(\mathbf{x}_k) - y_k)^2 + c \int_{\mathcal{X}} \int_{\mathcal{X}} u(\mathbf{x}, \mathbf{x}^\dagger) f(\mathbf{x}) f(\mathbf{x}^\dagger) d\mathbf{x} d\mathbf{x}^\dagger. \quad (13)$$

The variational problem (13) has appeared in machine learning context extensively [Girosi et al., 1995]. It has a known solution form, due to representer theorem [Schölkopf et al., 2001], which we will present here in a proposition. However, we first need to introduce some definitions. Let $g(\mathbf{x}, \mathbf{t})$ be a function such that,

$$\int_{\mathcal{X}} u(\mathbf{x}, \mathbf{x}^\dagger) g(\mathbf{x}^\dagger, \mathbf{t}) d\mathbf{x}^\dagger = \delta(\mathbf{x} - \mathbf{t}), \quad (14)$$

where $\delta(\mathbf{x})$ is Dirac delta. Such g is called the *Green's function*⁶ of the linear operator L , with L being $[Lf](\mathbf{x}) \triangleq \int_{\mathcal{X}} u(\mathbf{x}, \mathbf{x}^\dagger) f(\mathbf{x}^\dagger) d\mathbf{x}^\dagger$. Let the matrix $\mathbf{G}_{K \times K}$ and the vector $\mathbf{g}_{\mathbf{x} K \times 1}$ be defined as,

$$\mathbf{G}[j, k] \triangleq \frac{1}{K} g(\mathbf{x}_j, \mathbf{x}_k) \quad (15)$$

$$\mathbf{g}_{\mathbf{x}}[k] \triangleq \frac{1}{K} g(\mathbf{x}, \mathbf{x}_k). \quad (16)$$

Proposition 1 *The variational problem (13) has a solution of the form,*

$$f^*(\mathbf{x}) = \mathbf{g}_{\mathbf{x}}^T (\mathbf{c}\mathbf{I} + \mathbf{G})^{-1} \mathbf{y}. \quad (17)$$

⁶We assume that the Green's function exists and is continuous. Detailed treatment of existence conditions is beyond the scope of this work and can be found in text books such as [Duffy, 2001].

Notice that the matrix \mathbf{G} is *positive definite*⁷. Since by definition $c > 0$, the inverse of the matrix $c\mathbf{I} + \mathbf{G}$ is well-defined. Also, because \mathbf{G} is positive definite, it can be diagonalized as,

$$\mathbf{G} = \mathbf{V}^T \mathbf{D} \mathbf{V}, \quad (18)$$

where the diagonal matrix \mathbf{D} contains the eigenvalues of \mathbf{G} , denoted as d_1, \dots, d_K that are strictly greater than zero, and the matrix \mathbf{V} contains the corresponding eigenvectors.

2.3 Bounds on Multiplier c

Earlier we showed that any $c > 0$ that is a root of $\frac{1}{K} \sum_k (f_c^*(\mathbf{x}_k) - y_k)^2 - \epsilon = 0$ produces an optimal solution f^* via (13). However, in the settings that we are interested in, we do not know the underlying c or f^* beforehand; we have to relate them the given training data instead. As we will see later in Proposition 3, knowledge of c allows us to resolve the recurrence on \mathbf{y} created by self-distillation loop and obtain an explicit bound $\|\mathbf{y}\|$ at each distillation round. Unfortunately finding c in closed form by seeking roots of $\frac{1}{K} \sum_k (f_c^*(\mathbf{x}_k) - y_k)^2 - \epsilon = 0$ w.r.t. c is impossible, due to the nonlinear dependency of f on c caused by matrix inversion; see (17). However, we can still provide bounds on the value of c as shown in this section.

Throughout the analysis, it is sometimes easier to work with rotated labels $\mathbf{V}\mathbf{y}$. Thus we define,

$$\mathbf{z} \triangleq \mathbf{V}\mathbf{y}. \quad (19)$$

Note that any result on \mathbf{z} can be easily converted back via $\mathbf{y} = \mathbf{V}^T \mathbf{z}$, as \mathbf{V} is an orthogonal matrix. Trivially $\|\mathbf{z}\| = \|\mathbf{y}\|$. Our first step is to present a simplified form for the error term $\frac{1}{K} \sum_k (f^*(\mathbf{x}_k) - y_k)^2$ using the following proposition.

Proposition 2 *The following identity holds,*

$$\frac{1}{K} \sum_k (f^*(\mathbf{x}_k) - y_k)^2 = \frac{1}{K} \sum_k \left(z_k \frac{c}{c + d_k} \right)^2. \quad (20)$$

We now proceed to bound the roots of $h(c) \triangleq \frac{1}{K} \sum_k \left(z_k \frac{c}{c + d_k} \right)^2 - \epsilon$. Since we are considering $\|\mathbf{y}\|^2 > K\epsilon$, and thus by (10) $c > 0$, it is easy to construct the following lower and upper bounds on h ,

$$\underline{h}(c) \triangleq \frac{1}{K} \sum_k \left(z_k \frac{c}{c + d_{\max}} \right)^2 - \epsilon \quad (21)$$

$$\bar{h}(c) \triangleq \frac{1}{K} \sum_k \left(z_k \frac{c}{c + d_{\min}} \right)^2 - \epsilon. \quad (22)$$

The roots of \underline{h} and \bar{h} , namely c_1 and c_2 , can be easily derived,

$$c_1 = \frac{d_{\max} \sqrt{K\epsilon}}{\|\mathbf{z}\| - \sqrt{K\epsilon}}, \quad c_2 = \frac{d_{\min} \sqrt{K\epsilon}}{\|\mathbf{z}\| - \sqrt{K\epsilon}}. \quad (23)$$

Since $\underline{h}(c) \leq h(c)$, the condition $\underline{h}(c_1) = 0$ implies that $h(c_1) \geq 0$. Similarly, since $h(c) \leq \bar{h}(c)$, the condition $\bar{h}(c_2) = 0$ implies that $h(c_2) \leq 0$. By the intermediate value theorem, due to continuity of f and the fact that $\|\mathbf{z}\| = \|\mathbf{y}\| > \sqrt{K\epsilon}$ (non-collapse condition), there is a point c between c_1 and c_2 at which $h(c) = 0$,

$$\frac{d_{\min} \sqrt{K\epsilon}}{\|\mathbf{z}\| - \sqrt{K\epsilon}} \leq c \leq \frac{d_{\max} \sqrt{K\epsilon}}{\|\mathbf{z}\| - \sqrt{K\epsilon}}. \quad (24)$$

⁷This property of \mathbf{G} comes from the fact that u is a positive definite kernel (definite instead of semi-definite, due to empty null space assumption on the operator L), thus so is its inverse (i.e. g). Since g is a kernel, its associated Gram matrix is positive definite.

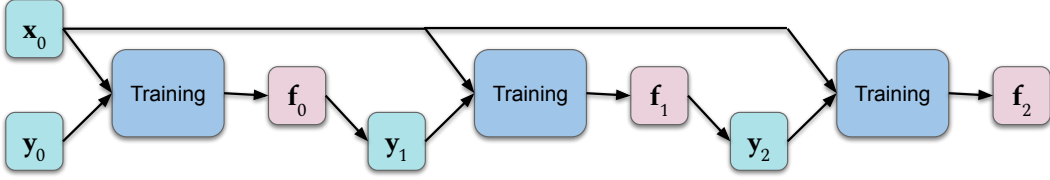


Figure 1: Schematic illustration of the self-distillation process for two iterations.

3 Self-Distillation

Denote the prediction vector over the training data $\mathbf{x}_1, \dots, \mathbf{x}_K$ as,

$$\mathbf{f}_{K \times 1} \triangleq [f^*(\mathbf{x}_1) | \dots | f^*(\mathbf{x}_K)]^T \quad (25)$$

$$= \mathbf{V}^T \mathbf{D} (c\mathbf{I} + \mathbf{D})^{-1} \mathbf{V} \mathbf{y}. \quad (26)$$

Self-distillation treats this prediction as target labels for a new round of training, and repeats this process as shown in Figure 1. With abuse of notation, denote the t 'th round of distillation by subscript t . We refer to the standard training (no self-distillation yet) by the step $t = 0$. Thus the standard training step has the form,

$$\mathbf{f}_0 = \mathbf{V}^T \mathbf{D} (c_0 \mathbf{I} + \mathbf{D})^{-1} \mathbf{V} \mathbf{y}_0, \quad (27)$$

where \mathbf{y}_0 is the ground truth labels as defined in (9). Letting $\mathbf{y}_1 \triangleq \mathbf{f}_0$, we achieve the next model by applying the first round of self-distillation,

$$\mathbf{f}_1 = \mathbf{V}^T \mathbf{D} (c_1 \mathbf{I} + \mathbf{D})^{-1} \mathbf{V} \mathbf{y}_1, \quad (28)$$

In general, for any $t \geq 1$ we have the following recurrence,

$$\mathbf{y}_t = \mathbf{V}^T \mathbf{A}_{t-1} \mathbf{V} \mathbf{y}_{t-1}, \quad (29)$$

where we define for any $t \geq 0$,

$$\mathbf{A}_{t, K \times K} \triangleq \mathbf{D} (c_t \mathbf{I} + \mathbf{D})^{-1}. \quad (30)$$

Note that \mathbf{A}_t is also a diagonal matrix. Furthermore, since at the t 'th distillation step, everything is the same as the initial step except the training labels, we can use Proposition 1 to express $f_t(\mathbf{x})$ as,

$$f_t^*(\mathbf{x}) = \mathbf{g}_x^T (c_t \mathbf{I} + \mathbf{G})^{-1} \mathbf{y}_t = \mathbf{g}_x^T \mathbf{V}^T (\prod_{i=0}^t \mathbf{A}_i) \mathbf{V} \mathbf{y}_0. \quad (31)$$

Observe that the only dynamic component in the expression of f_t^* is $\prod_{i=0}^t \mathbf{A}_i$. In the following, we show how $\prod_{i=0}^t \mathbf{A}_i$ evolves over time. Specifically, we show that self-distillation progressively sparsifies the matrix $\prod_{i=0}^t \mathbf{A}_i$ at a provided rate.

Also recall from Section 2.1 that *in each step of self-distillation* we require $\|\mathbf{y}_t\| > \sqrt{K} \epsilon$. If this condition breaks at any point, the solution *collapses* to the zero function, and subsequent rounds of self-distillation keep producing $f^*(\mathbf{x}) = 0$. In this section we present a lower bound on number of iterations t that guarantees all intermediate problems satisfy $\|\mathbf{y}_t\| > \sqrt{K} \epsilon$.

3.1 Unfolding the Recurrence

Our goal here is to understand how $\|\mathbf{y}_t\|$ evolves in t . By combining (29) and (30) we obtain,

$$\mathbf{y}_t = \mathbf{V}^T \mathbf{D} (c_{t-1} \mathbf{I} + \mathbf{D})^{-1} \mathbf{V} \mathbf{y}_{t-1}. \quad (32)$$

By multiplying both sides from the left by \mathbf{V} we get,

$$\mathbf{V}\mathbf{y}_t = \mathbf{V}\mathbf{V}^T \mathbf{D}(c_{t-1}\mathbf{I} + \mathbf{D})^{-1} \mathbf{V}\mathbf{y}_{t-1} \quad (33)$$

$$\equiv \mathbf{z}_t = \mathbf{D}(c_{t-1}\mathbf{I} + \mathbf{D})^{-1} \mathbf{z}_{t-1} \quad (34)$$

$$\equiv \frac{1}{\sqrt{K}\epsilon} \mathbf{z}_t = \mathbf{D}(c_{t-1}\mathbf{I} + \mathbf{D})^{-1} \frac{1}{\sqrt{K}\epsilon} \mathbf{z}_{t-1}. \quad (35)$$

Also we can use the bounds on c from (24) at any arbitrary $t \geq 0$ and thus write,

$$\forall t \geq 0; \|\mathbf{z}_t\| > \sqrt{K}\epsilon \Rightarrow \frac{d_{\min}\sqrt{K}\epsilon}{\|\mathbf{z}_t\| - \sqrt{K}\epsilon} \leq c_t \leq \frac{d_{\max}\sqrt{K}\epsilon}{\|\mathbf{z}_t\| - \sqrt{K}\epsilon} \quad (36)$$

By combining (35) and (36) we obtain a recurrence solely in \mathbf{z} ,

$$\mathbf{z}_t = \mathbf{D}\left(\frac{\alpha_t\sqrt{K}\epsilon}{\|\mathbf{z}_{t-1}\| - \sqrt{K}\epsilon}\mathbf{I} + \mathbf{D}\right)^{-1} \mathbf{z}_{t-1}, \quad (37)$$

where,

$$d_{\min} \leq \alpha_t \leq d_{\max}. \quad (38)$$

We now establish a lower bound on the value of $\|\mathbf{z}_t\|$.

Proposition 3 For any $t \geq 0$, if $\|\mathbf{z}_i\| > \sqrt{K}\epsilon$ for $i = 0, \dots, t$, then,

$$\|\mathbf{z}_t\| \geq a^t(\kappa)\|\mathbf{z}_0\| - \sqrt{K}\epsilon b(\kappa) \frac{a^t(\kappa) - 1}{a(\kappa) - 1}, \quad (39)$$

where,

$$a(x) \triangleq \frac{(r_0 - 1)^2 + x(2r_0 - 1)}{(r_0 - 1 + x)^2} \quad (40)$$

$$b(x) \triangleq \frac{r_0^2 x}{(r_0 - 1 + x)^2} \quad (41)$$

$$r_0 \triangleq \frac{1}{\sqrt{K}\epsilon} \|\mathbf{z}_0\|, \quad \kappa \triangleq \frac{d_{\max}}{d_{\min}}. \quad (42)$$

3.2 Guaranteed Number of Self-Distillation Rounds

By looking at (34) it is not hard to see the value of $\|\mathbf{z}_t\|$ is *decreasing* in t . That is because c_t ⁸ as well as elements of the diagonal matrix \mathbf{D} are strictly positive. Hence $\mathbf{D}(c_{t-1}\mathbf{I} + \mathbf{D})^{-1}$ shrinks the magnitude of \mathbf{z}_{t-1} in each iteration.

Thus, starting from $\|\mathbf{z}_0\| > \sqrt{K}\epsilon$, as $\|\mathbf{z}_t\|$ decreases, at some point it falls below the value $\sqrt{K}\epsilon$ and thus the solution collapses. We now want to find out after how many rounds t , the solution collapse happens. Finding the exact such t , is difficult, but by setting a lower bound of $\|\mathbf{z}_t\|$ to $\sqrt{K}\epsilon$ and solving that in t , calling the solution \underline{t} , we can guarantee realization of at least \underline{t} rounds where the value of $\|\mathbf{z}_{\underline{t}}\|$ remains above $\sqrt{K}\epsilon$.

We can use the lower bound we developed in Proposition 3 in order to find such \underline{t} . This is shown in the following proposition.

⁸ $c_t > 0$ following from the assumption $\|\mathbf{z}_t\| > \sqrt{K}\epsilon$ and (10).

Proposition 4 Starting from $\|\mathbf{y}_0\| > \sqrt{K}\epsilon$, meaningful (non-collapsing solution) self-distillation is possible at least for \underline{t} rounds,

$$\underline{t} \triangleq \frac{\frac{\|\mathbf{y}_0\|}{\sqrt{K}\epsilon} - 1}{\kappa}. \quad (43)$$

Note that when we are in near-interpolation regime, i.e. $\epsilon \rightarrow 0$, the form of \underline{t} simplifies: $\underline{t} \approx \frac{\|\mathbf{y}_0\|}{\kappa\sqrt{K}\epsilon}$.

3.3 Evolution of Basis

Recall from (31) that the learned function after t rounds of self-distillation has the form,

$$f_t^*(\mathbf{x}) = \mathbf{g}_x^T \mathbf{V}^T (\Pi_{i=0}^t \mathbf{A}_t) \mathbf{V} \mathbf{y}_0. \quad (44)$$

The only time-dependent part is thus the following *diagonal* matrix,

$$\mathbf{B}_t \triangleq \Pi_{i=0}^t \mathbf{A}_t. \quad (45)$$

In this section we show how \mathbf{B}_t evolves over time. Specifically, we claim that the matrix \mathbf{B}_t becomes progressively sparser as t increases.

Proposition 5 Suppose $\|\mathbf{y}_0\| > \sqrt{K}\epsilon$ and $t \leq \frac{\|\mathbf{y}_0\|}{\kappa\sqrt{K}\epsilon} - \frac{1}{\kappa}$. Then for any pair of diagonals of \mathbf{D} , namely d_j and d_k , with the condition that $d_k > d_j$, the following inequality holds.

$$\frac{\mathbf{B}_{t-1}[k, k]}{\mathbf{B}_{t-1}[j, j]} \geq \left(\frac{\frac{\|\mathbf{y}_0\|}{\sqrt{K}\epsilon} - 1 + \frac{d_{\min}}{d_j}}{\frac{\|\mathbf{y}_0\|}{\sqrt{K}\epsilon} - 1 + \frac{d_{\min}}{d_k}} \right)^t. \quad (46)$$

The above proposition suggests that, as t increases, the smaller elements of \mathbf{B}_{t-1} shrink faster and at some point become negligible compared to larger ones. That is because in (46) we have assumed $d_k > d_j$, and thus the r.h.s. expression in the parentheses is strictly greater than 1. The latter implies that $\frac{\mathbf{B}_{t-1}[k, k]}{\mathbf{B}_{t-1}[j, j]}$ is increasing in t .

Observe that if one was able to push $t \rightarrow \infty$, then only one entry of \mathbf{B}_t (the one corresponding to d_{\max}) would remain significant relative to others. Thus, self-distillation process *progressively sparsifies* \mathbf{B}_t . This sparsification affects the expressiveness of the regression solution $f_t^*(\mathbf{x})$. To see that, use the definition of $f_t^*(\mathbf{x})$ from (31) to express it in the following form,

$$f_t^*(\mathbf{x}) = \mathbf{g}_x^T \mathbf{V}^T \mathbf{B}_t \mathbf{V} \mathbf{y}_0 = \mathbf{p}_x^T \mathbf{B}_t \mathbf{z}_0. \quad (47)$$

where we gave a name to the rotated basis $\mathbf{p}_x \triangleq \mathbf{V} \mathbf{g}_x$ and rotated vector $\mathbf{z}_0 \triangleq \mathbf{V} \mathbf{y}_0$. The solution f_t^* is essentially represented by a weighted sum of the basis functions (the components of \mathbf{p}_x). Thus, the number of significant diagonal entries of \mathbf{B}_t determines the *effective number of basis functions* used to represent the solution.

3.4 Self-Distillation vs Early Stopping

Broadly speaking, early stopping can be interpreted as any procedure that cuts convergence short of the optimal solution. Examples include reducing the number of iterations of the numerical optimizer (e.g. SGD), or increasing the loss tolerance threshold ϵ . The former is not applicable to our setting, as our analysis is independent of function parametrization and its numerical optimization. We consider the second definition.

This form of early stopping also has a regularization effect; by increasing ϵ in (1) the feasible set expands and thus it is possible to find functions with lower $R(f)$. However, we show here that the induced regularization is not equivalent to that of self-distillation. In fact, one can say that early-stopping does the *opposite* of sparsification, as we show below.

The learned function via loss-based early stopping in our notation can be expressed as f_0^* (single training, no self-distillation) with a larger error tolerance ϵ ,

$$f_0^*(\mathbf{x}) = \mathbf{p}_x^T \mathbf{B}_0 \mathbf{z}_0 = \mathbf{p}_x^T \mathbf{D}(c_0 \mathbf{I} + \mathbf{D})^{-1} \mathbf{z}_0. \quad (48)$$

The effect of larger ϵ on the value of c_0 is shown in (24). However, since c_0 is just a scalar value applied to matrices, it does not provide any lever to increase the sparsity of \mathbf{D} . We now elaborate on the latter claim a bit more. Observe that, on the one hand, when c_0 is large, then $\mathbf{D}(c_0 \mathbf{I} + \mathbf{D})^{-1} \approx \frac{1}{c_0} \mathbf{D}$, which essentially uses \mathbf{D} and does not sparsify it further. On the other hand, if c_0 is small then $\mathbf{D}(c_0 \mathbf{I} + \mathbf{D})^{-1} \approx \mathbf{I}$, which is the densest possible diagonal matrix. Thus, at best, early stopping maintains the original sparsity pattern of \mathbf{D} and otherwise makes it even denser.

3.5 Advantage of Near Interpolation Regime

As discussed in Section (3.3), one can think of $\frac{\mathbf{B}_{t-1}[k,k]}{\mathbf{B}_{t-1}[j,j]}$ as a sparsity measure (the larger, the sparser). Thus, we define a *sparsity index* based on the lower bound we developed for $\frac{\mathbf{B}_{t-1}[k,k]}{\mathbf{B}_{t-1}[j,j]}$ in Proposition 5. In fact, by finding the lowest value of the bound across elements all elements satisfying $d_k > d_j$, we can ensure all pairs to reach at least the sparsity level of,

$$S_{\mathbf{B}_{t-1}} \triangleq \min_{j,k} \left(\frac{\frac{\|\mathbf{y}_0\|}{\sqrt{K}\epsilon} - 1 + \frac{d_{\min}}{d_j}}{\frac{\|\mathbf{y}_0\|}{\sqrt{K}\epsilon} - 1 + \frac{d_{\min}}{d_k}} \right)^t \quad \text{s.t.} \quad d_k > d_j. \quad (49)$$

Assuming d 's are ordered so that $d_1 < d_2 < \dots < d_K$ then the above simplifies to,

$$S_{\mathbf{B}_{t-1}} = \min_{k \in \{1, 2, \dots, K-1\}} \left(\frac{\frac{\|\mathbf{y}_0\|}{\sqrt{K}\epsilon} - 1 + \frac{d_{\min}}{d_k}}{\frac{\|\mathbf{y}_0\|}{\sqrt{K}\epsilon} - 1 + \frac{d_{\min}}{d_{k+1}}} \right)^t. \quad (50)$$

One may wonder what is the highest sparsity S that self-distillation can attain. Since $\|\mathbf{y}_0\| > \sqrt{K}\epsilon$ and $d_{k+1} > d_k$, the term inside parentheses in (50) is strictly greater than 1 and thus S increases in t . However, the largest t we can guarantee before a solution collapse happens (provided in Proposition 4) is $\underline{t} = \frac{\|\mathbf{y}_0\|}{\kappa\sqrt{K}\epsilon} - \frac{1}{\kappa}$. By plugging this \underline{t} into the definition of S from (50) we eliminate t and obtain the largest sparsity index,

$$S_{\mathbf{B}_{\underline{t}-1}} = \min_{k \in \{1, 2, \dots, K-1\}} \left(\frac{\frac{\|\mathbf{y}_0\|}{\sqrt{K}\epsilon} - 1 + \frac{d_{\min}}{d_k}}{\frac{\|\mathbf{y}_0\|}{\sqrt{K}\epsilon} - 1 + \frac{d_{\min}}{d_{k+1}}} \right)^{\frac{\|\mathbf{y}_0\|}{\kappa\sqrt{K}\epsilon} - \frac{1}{\kappa}}. \quad (51)$$

We now further show that $S_{\mathbf{B}_{\underline{t}-1}}$ always improves as ϵ gets smaller.

Proposition 6 Suppose $\|\mathbf{y}_0\| > \sqrt{K}\epsilon$. Then the sparsity index $S_{\mathbf{B}_{\underline{t}-1}}$ (where $\underline{t} = \frac{\|\mathbf{y}_0\|}{\kappa\sqrt{K}\epsilon} - \frac{1}{\kappa}$ is number of guaranteed self-distillation steps before solution collapse) *decreases* in ϵ , i.e. lower ϵ yields higher sparsity.

Furthermore at the limit $\epsilon \rightarrow 0$, the sparsity index has the form,

$$\lim_{\epsilon \rightarrow 0} S_{\mathbf{B}_{\underline{t}-1}} = e^{\frac{d_{\min}}{\kappa} \min_{k \in \{1, 2, \dots, K-1\}} \left(\frac{1}{d_k} - \frac{1}{d_{k+1}} \right)}. \quad (52)$$

Thus, if high sparsity is a desired goal, one should choose ϵ as small as possible. One should however note that the value of ϵ cannot be *identically zero*, i.e. exact interpolation regime, because then $\mathbf{f}_0 = \mathbf{y}_0$, and since $\mathbf{y}_1 = \mathbf{f}_0$, self-distillation process keeps producing the same model in each round.

3.6 Multiclass Extension

We can formulate multiclass classification, by regressing to a one-hot encoding. Specifically, a problem with Q classes can be modeled by Q output functions f_1, \dots, f_Q . An easy extension of our analysis to this multiclass setting is to require the functions f_1, \dots, f_Q be smooth by applying the same regularization R to each and then adding up these regularization terms. This way, the optimal function for each output unit can be solved for each $q = 1, \dots, Q$

$$f_q^* \triangleq \arg \min_{f_q \in \mathcal{F}} \frac{1}{K} \sum_k \left(f_q(\mathbf{x}_k) - y_{qk} \right)^2 + c_q R(f_q). \quad (53)$$

4 Illustrative Example

Let \mathcal{F} be the space of twice differentiable functions that map $[0, 1]$ to \mathbb{R} ,

$$\mathcal{F} \triangleq \{f \mid f : [0, 1] \rightarrow \mathbb{R}\}. \quad (54)$$

Define the linear operator $P : \mathcal{F} \rightarrow \mathcal{F}$ as,

$$[Pf](x) \triangleq \frac{d^2}{dx^2} f(x), \quad (55)$$

subject to boundary conditions,

$$f(0) = f(1) = f''(0) = f''(1) = 0. \quad (56)$$

The associated regularization functional becomes,

$$R(f) \triangleq \int_0^1 \left(\frac{d^2}{dx^2} f(x) \right)^2 dx. \quad (57)$$

Observe that this regularizer encourages smoother f by penalizing the second order derivative of the function. The Green's function of the operator associated with the kernel of R subject to the listed boundary conditions is a spline with the following form [Rytgaard, 2016] (see Figure 2-a),

$$g(x, x^\dagger) = \frac{1}{6} \max((x - x^\dagger)^3, 0) - \frac{1}{6} x(1 - x^\dagger)(x^2 - 2x^\dagger + x^{\dagger 2}). \quad (58)$$

Now consider training points (x_k, y_k) sampled from the function $y = \sin(2\pi x)$. Let x_k be evenly spaced in the interval $[0, 1]$ with steps of 0.1, and $y_k = x_k + \eta$ where η is a zero-mean normal random variable with $\sigma = 0.5$ (Figure 2-b).

As shown in Figure 2-c, the regularization induced by self-distillation initially improves the quality of the fit, but after that point additional rounds of self-distillation over-regularize and lead to underfitting.

We also computed the diagonal matrix \mathbf{B}_t (see (45) for definition) at each self-distillation round t , for $t = 0, \dots, 3$ (after that, the solution collapses). Recall from (47) that the entries of this matrix can be thought of as the coefficients of basis functions used to represent the solution. As predicted by our analysis, self-distillation regularizes the solution by sparsifying these coefficients. This is evident in Figure 3 where smaller coefficients shrink faster.

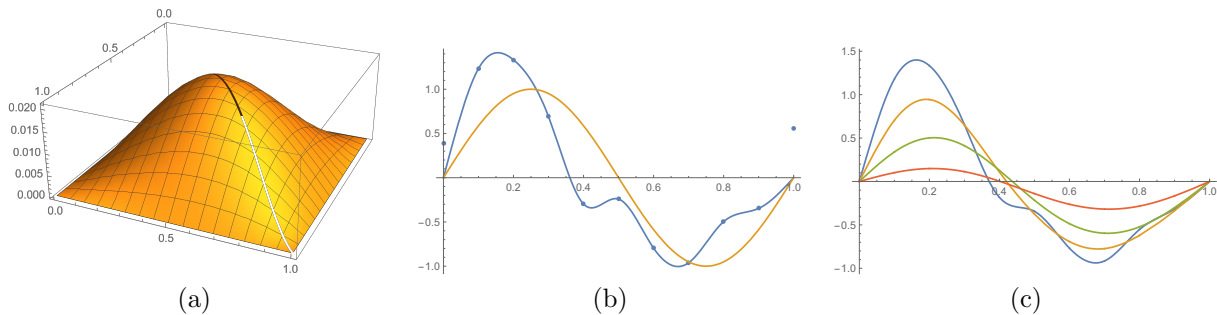


Figure 2: Example with $R(f)(x) \triangleq \int_0^1 \left(\frac{d^2}{dx^2} f(x)\right)^2 dx$. (a) Green's function associated with the kernel of R . (b) Noisy training samples (blue dots) from underlying function (orange) $y = \sin(2\pi x)$. Fitting without regularization leads to overfitting (blue curve). (c) Four rounds of self-distillation (blue, orange, green, red) with $\epsilon = 0.04$.

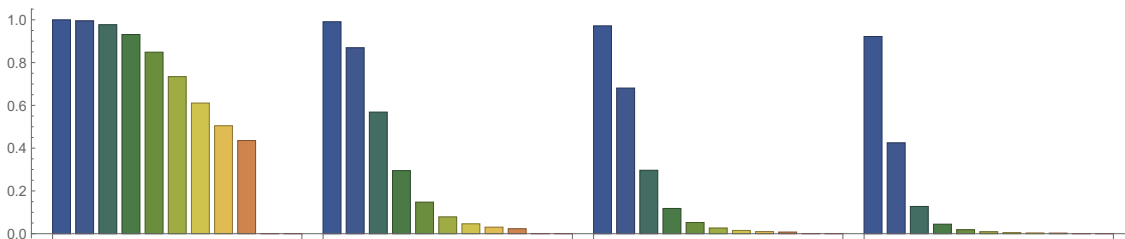


Figure 3: Evolution of the diagonal entries of (the diagonal matrix) \mathbf{B}_t from (45) at distillation rounds $t = 0$ (left most) to $t = 3$ (right most). The number of training points is $K = 11$, so \mathbf{B}_t which is $K \times K$ diagonal matrix has 11 entries on its diagonal, each corresponding to one of the bars in the chart.

5 Experiments

5.1 Motivation

Recent works on the Neural Tangent Kernel (NTK) [Jacot et al., 2018] have shown that training deep models with infinite width and ℓ_2 loss (and small step size for optimization) is equivalent to performing *kernel regression* with a specific kernel. The kernel function, which is outer product of network’s Jacobian matrix, encodes various biases induced by the architecture (convolution, pooling, nested representations, etc.) that enable the deep models generalize well despite its high capacity.

The regularization form (2) that we studied here also reduces to a kernel regression problem, with the kernel being the Green’s function of the regularizer. In fact, regularized regression (1) and kernel regression can be converted to each other [Smola et al., 1998] and thus, in principle, one can convert an NTK kernel into a regularizer of form (2). This implies that at least in the NTK regime of neural networks, our analysis can provide a reasonable representation of self-distillation.

Of course, real architectures have finite width and thus the NTK (and consequently our self-distillation analysis) may not always be a faithful approximation. However, the growing literature on NTK is showing scenarios where this regime is still valid under large width [Lee et al., 2019], particular choices of scaling between the weights and the inputs [Chizat et al., 2019], and for fully connected networks [Geiger et al., 2019].

We hope our analysis can provide some insight into how self-distillation dynamic affects generalization. For example, the model may benefit from stronger regularizer encoded by the underlying regularizer (or equivalently kernel), and thus improve on test performance initially. However, as we discussed, excessive self-distillation can over regularize the model and thus lead to underfitting. According to this picture, the test accuracy may first go up but then will go down (instead of approaching its best value, for example). Our empirical results on deep models follow this pattern.

5.2 Results

Setup. We use Resnet [He et al., 2015] and VGG [Simonyan and Zisserman, 2015] neural architectures and train them on CIFAR-10 and CIFAR-100 datasets [Krizhevsky, 2009]. Training details and additional results are left to the appendix. Each curve in the plots corresponds to 10 runs from randomly initialized weights, where each run is a chain of self-distillation steps. In the plot, a point represents the average and the envelope around it reflects standard deviation. Any training accuracy reported here is based on assessing the model f_t at the t ’th self-distillation round on the *original* training labels \mathbf{y}_0 .

ℓ_2 Loss on Neural Network Predictions. Here we train the neural network using ℓ_2 loss. The error is defined as the difference between predictions (softmax over the logits) and the target labels. These results are in concordance with a regularization viewpoint of self-distillation. The theory suggests that self-distillation progressively amplifies the underlying regularization effect. As such, we expect the training accuracy (over \mathbf{y}_0) to drop in each self-distillation round. Test accuracy may go up if training can benefit from amplified regularization. However, from the theory we expect the test accuracy to go down at some point due to over regularization and thus underfitting. Both of these phenomena are observed in Figure 4.

Cross Entropy Loss on Neural Network Predictions. Although, our theory only applies to ℓ_2 , loss, we empirically observed similar phenomena for cross entropy as shown in Figure 5.

Self-Distillation $\not\approx$ Early Stopping. By looking at the fall of the training accuracy over self-distillation round, one may wonder if early stopping (in the sense of choosing a larger error tolerance ϵ for training) would lead to similar test performance. However, In Section 3.4 we discussed that self-distillation and early stopping have different regularization effects. Here we try to verify that.

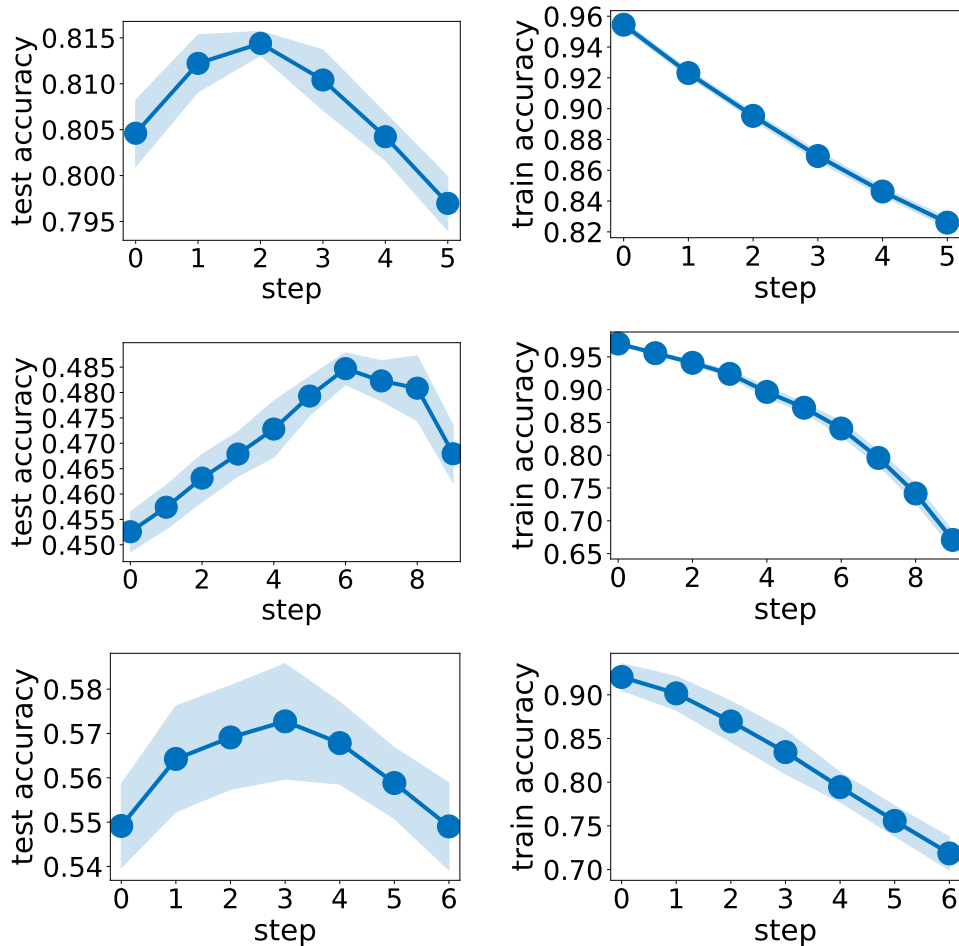


Figure 4: Self-distillation with ℓ_2 loss on neural network predictions for: (top) Resnet50 on CIFAR-10, (middle) Resnet50 on CIFAR-100, (bottom) VGG16 on CIFAR-100.

Specifically, we record the training loss value at the end of each self-distillation round. We then train a batch of models from scratch until each batch converges to one of the recorded loss values. If the regularization induced by early stopping was the same as self-distillation, then we should have seen similar test performance between a self-distilled model that achieves a specific loss value on the original training labels, and a model that stops training as soon as it reaches the same level of error. However, as shown in Figure 6, the two have different regularization effects.

6 Conclusion

In this work, we presented a rigorous analysis of self-distillation for regularized regression in a Hilbert space of functions. We showed that self-distillation iterations in the setting we studied cannot continue indefinitely; at some point the solution collapses to zero. We provided a lower bound on the number of meaningful (non-collapsed) distillation iterations. In addition, we proved that self-distillation acts as a regularizer that progressively employs fewer basis functions for representing the solution. We discussed the difference in regularization effect induced by self-distillation against early stopping. We also showed that operating in near-interpolation regime facilitates the regularization effect. We discussed how our

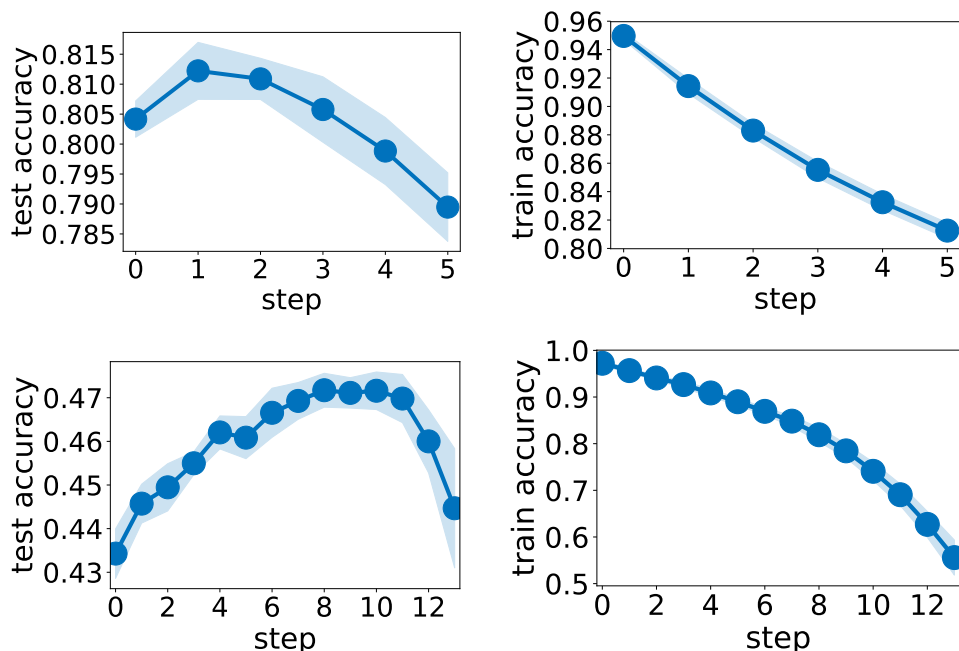


Figure 5: Self-distillation with cross entropy loss on predictions for Resnet50 (top) on CIFAR-10, (bottom) on CIFAR-100.

regression setting resembles the NTK view of wide neural networks, and thus may provide some insight into how self-distillation works in deep learning.

We hope that our work can be used as a stepping stone to broader settings. In particular, studying cross-entropy loss as well as other forms of regularization are interesting directions for further research.

7 Acknowledgement

We would like to thank colleagues at Google Research for their feedback and comments: Moshe Dubiner, Pierre Foret, Sergey Ioffe, Yiding Jiang, Alan MacKey, Matt Streeter, and Andrey Zhmoginov.

References

- [Ahn et al., 2019] Ahn, S., Hu, S. X., Damianou, A. C., Lawrence, N. D., and Dai, Z. (2019). Variational information distillation for knowledge transfer. *2019 IEEE/CVF Conference on Computer Vision and Pattern Recognition (CVPR)*, pages 9155–9163.
- [Chizat et al., 2019] Chizat, L., Oyallon, E., and Bach, F. (2019). On lazy training in differentiable programming. In *Advances in Neural Information Processing Systems 32*, pages 2933–2943. Curran Associates, Inc.
- [Dong et al., 2019] Dong, B., Hou, J., Lu, Y., and Zhang, Z. (2019). Distillation early stopping? harvesting dark knowledge utilizing anisotropic information retrieval for overparameterized neural network. *ArXiv*, abs/1910.01255.
- [Duffy, 2001] Duffy, D. (2001). *Green’s Functions with Applications*. Applied Mathematics. CRC Press.

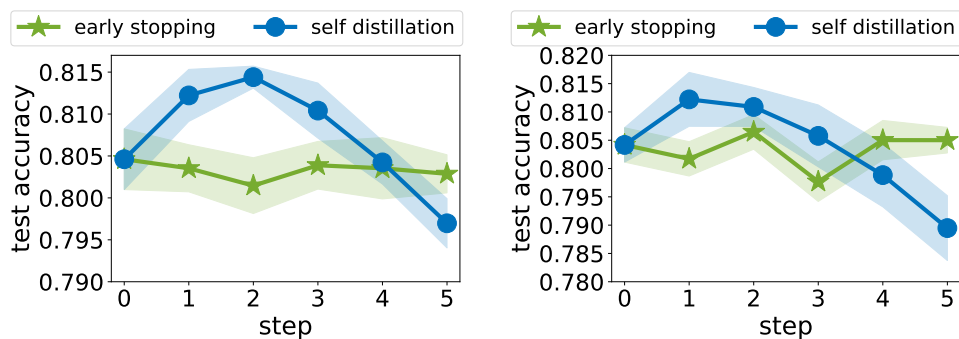


Figure 6: Self-distillation compared to early stopping for Resnet50 and CIFAR-10 on (left) ℓ_2 loss (right) cross entropy loss.

- [Furlanello et al., 2018] Furlanello, T., Lipton, Z. C., Tschannen, M., Itti, L., and Anandkumar, A. (2018). Born-again neural networks. In *Proceedings of the 35th International Conference on Machine Learning, ICML 2018, Stockholmsmässan, Stockholm, Sweden, July 10-15, 2018*, pages 1602–1611.
- [Geiger et al., 2019] Geiger, M., Spigler, S., Jacot, A., and Wyart, M. (2019). Disentangling feature and lazy training in deep neural networks. *arXiv e-prints*, page arXiv:1906.08034.
- [Ghosh et al., 2018] Ghosh, D., Singh, A., Rajeswaran, A., Kumar, V., and Levine, S. (2018). Divide-and-conquer reinforcement learning. In *International Conference on Learning Representations*.
- [Girosi et al., 1995] Girosi, F., Jones, M., and Poggio, T. (1995). Regularization theory and neural networks architectures. *Neural Computation*, 7(2):219–269.
- [Gotmare et al., 2019] Gotmare, A., Keskar, N. S., Xiong, C., and Socher, R. (2019). A closer look at deep learning heuristics: Learning rate restarts, warmup and distillation. In *International Conference on Learning Representations*.
- [He et al., 2015] He, K., Zhang, X., Ren, S., and Sun, J. (2015). Deep residual learning for image recognition. *2016 IEEE Conference on Computer Vision and Pattern Recognition (CVPR)*, pages 770–778.
- [Hinton et al., 2015] Hinton, G., Vinyals, O., and Dean, J. (2015). Distilling the knowledge in a neural network. In *NIPS Deep Learning and Representation Learning Workshop*.
- [Hong et al., 2020] Hong, Z.-W., Nagarajan, P., and Maeda, G. (2020). Collaborative inter-agent knowledge distillation for reinforcement learning.
- [Huang and Wang, 2017] Huang, Z. and Wang, N. (2017). Like what you like: Knowledge distill via neuron selectivity transfer. *CoRR*, abs/1707.01219.
- [Jacot et al., 2018] Jacot, A., Gabriel, F., and Hongler, C. (2018). Neural tangent kernel: Convergence and generalization in neural networks. In *Proceedings of the 32Nd International Conference on Neural Information Processing Systems, NIPS’18*, pages 8580–8589, USA. Curran Associates Inc.
- [Korattikara Balan et al., 2015] Korattikara Balan, A., Rathod, V., Murphy, K. P., and Welling, M. (2015). Bayesian dark knowledge. In Cortes, C., Lawrence, N. D., Lee, D. D., Sugiyama, M., and Garnett, R., editors, *Advances in Neural Information Processing Systems 28*, pages 3438–3446. Curran Associates, Inc.
- [Krizhevsky, 2009] Krizhevsky, A. (2009). Learning multiple layers of features from tiny images.

- [lan et al., 2018] lan, x., Zhu, X., and Gong, S. (2018). Knowledge distillation by on-the-fly native ensemble. In Bengio, S., Wallach, H., Larochelle, H., Grauman, K., Cesa-Bianchi, N., and Garnett, R., editors, *Advances in Neural Information Processing Systems 31*, pages 7517–7527. Curran Associates, Inc.
- [Lee et al., 2019] Lee, J., Xiao, L., Schoenholz, S., Bahri, Y., Novak, R., Sohl-Dickstein, J., and Pennington, J. (2019). Wide neural networks of any depth evolve as linear models under gradient descent. In *Advances in Neural Information Processing Systems 32*, pages 8570–8581. Curran Associates, Inc.
- [Li and Hoiem, 2016] Li, Z. and Hoiem, D. (2016). Learning without forgetting. In *ECCV*.
- [Mirzadeh et al., 2020] Mirzadeh, S., Farajtabar, M., Li, A., Levine, N., Matsukawa, A., and Ghasemzadeh, H. (2020). Improved knowledge distillation via teacher assistant: Bridging the gap between student and teacher. *AAAI 2020*, abs/1902.03393.
- [Nayak et al., 2019] Nayak, G. K., Mopuri, K. R., Shaj, V., Radhakrishnan, V. B., and Chakraborty, A. (2019). Zero-shot knowledge distillation in deep networks. In Chaudhuri, K. and Salakhutdinov, R., editors, *Proceedings of the 36th International Conference on Machine Learning*, volume 97 of *Proceedings of Machine Learning Research*, pages 4743–4751, Long Beach, California, USA. PMLR.
- [Park et al., 2019] Park, W., Kim, D., Lu, Y., and Cho, M. (2019). Relational knowledge distillation. *2019 IEEE/CVF Conference on Computer Vision and Pattern Recognition (CVPR)*, pages 3962–3971.
- [Romero et al., 2014] Romero, A., Ballas, N., Kahou, S. E., Chassang, A., Gatta, C., and Bengio, Y. (2014). Fitnets: Hints for thin deep nets. *CoRR*, abs/1412.6550.
- [Rytgaard, 2016] Rytgaard, H. C. (2016). Statistical models for robust spline smoothing. Master’s thesis, University of Copenhagen.
- [Schölkopf et al., 2001] Schölkopf, B., Herbrich, R., and Smola, A. (2001). A generalized representer theorem. In *Lecture Notes in Computer Science, Vol. 2111*, number 2111 in LNCS, pages 416–426, Berlin, Germany. Max-Planck-Gesellschaft, Springer.
- [Simonyan and Zisserman, 2015] Simonyan, K. and Zisserman, A. (2015). Very deep convolutional networks for large-scale image recognition. In *International Conference on Learning Representations*.
- [Smola et al., 1998] Smola, A., Schölkopf, B., and Müller, K.-R. (1998). The connection between regularization operators and support vector kernels. *Neural Networks*, 11(4):637–649.
- [Srinivas and Fleuret, 2018] Srinivas, S. and Fleuret, F. (2018). Knowledge transfer with jacobian matching. *CoRR*, abs/1803.00443.
- [Teh et al., 2017] Teh, Y., Bapst, V., Czarnecki, W. M., Quan, J., Kirkpatrick, J., Hadsell, R., Heess, N., and Pascanu, R. (2017). Distral: Robust multitask reinforcement learning. In Guyon, I., Luxburg, U. V., Bengio, S., Wallach, H., Fergus, R., Vishwanathan, S., and Garnett, R., editors, *Advances in Neural Information Processing Systems 30*, pages 4496–4506. Curran Associates, Inc.
- [Tran et al., 2020] Tran, L., Veeling, B. S., Roth, K., Swiatkowski, J., Dillon, J. V., Snoek, J., Mandt, S., Salimans, T., Nowozin, S., and Jenatton, R. (2020). Hydra: Preserving ensemble diversity for model distillation.
- [Vadera and Marlin, 2020] Vadera, M. P. and Marlin, B. M. (2020). Generalized bayesian posterior expectation distillation for deep neural networks.

- [Wang et al., 2018] Wang, X., Zhang, R., Sun, Y., and Qi, J. (2018). Kdgan: Knowledge distillation with generative adversarial networks. In Bengio, S., Wallach, H., Larochelle, H., Grauman, K., Cesa-Bianchi, N., and Garnett, R., editors, *Advances in Neural Information Processing Systems 31*, pages 775–786. Curran Associates, Inc.
- [Yang et al., 2019] Yang, C., Xie, L., Qiao, S., and Yuille, A. L. (2019). Training deep neural networks in generations: A more tolerant teacher educates better students. In *The Thirty-Third AAAI Conference on Artificial Intelligence, AAAI 2019, The Thirty-First Innovative Applications of Artificial Intelligence Conference, IAAI 2019, The Ninth AAAI Symposium on Educational Advances in Artificial Intelligence, EAAI 2019, Honolulu, Hawaii, USA, January 27 - February 1, 2019*, pages 5628–5635. AAAI Press.
- [Yim et al., 2017] Yim, J., Joo, D., Bae, J., and Kim, J. (2017). A gift from knowledge distillation: Fast optimization, network minimization and transfer learning. *2017 IEEE Conference on Computer Vision and Pattern Recognition (CVPR)*, pages 7130–7138.
- [Zhang et al., 2016] Zhang, C., Bengio, S., Hardt, M., Recht, B., and Vinyals, O. (2016). Understanding deep learning requires rethinking generalization. *arXiv preprint arXiv:1611.03530*.

A Solving the Variational Problem

In this section we derive the solution to the following variational problem,

$$f^* \triangleq \arg \min_{f \in \mathcal{F}} \frac{1}{K} \sum_k \left(f(\mathbf{x}_k) - y_k \right)^2 + c \int_{\mathcal{X}} \int_{\mathcal{X}} u(\mathbf{x}, \mathbf{x}^\dagger) f(\mathbf{x}) f(\mathbf{x}^\dagger) d\mathbf{x} d\mathbf{x}^\dagger. \quad (59)$$

Using Dirac delta function, we can rewrite the objective function as,

$$f^* = \arg \min_{f \in \mathcal{F}} \frac{1}{K} \sum_k \left(\int_{\mathcal{X}} f(\mathbf{x}) \delta(\mathbf{x} - \mathbf{x}_k) d\mathbf{x} - y_k \right)^2 + c \int_{\mathcal{X}} \int_{\mathcal{X}} u(\mathbf{x}, \mathbf{x}^\dagger) f(\mathbf{x}) f(\mathbf{x}^\dagger) d\mathbf{x} d\mathbf{x}^\dagger. \quad (60)$$

For brevity, name the objective functional J ,

$$J(f) \triangleq \frac{1}{K} \sum_k \left(\int_{\mathcal{X}} f(\mathbf{x}) \delta(\mathbf{x} - \mathbf{x}_k) d\mathbf{x} - y_k \right)^2 + c \int_{\mathcal{X}} \int_{\mathcal{X}} u(\mathbf{x}, \mathbf{x}^\dagger) f(\mathbf{x}) f(\mathbf{x}^\dagger) d\mathbf{x} d\mathbf{x}^\dagger. \quad (61)$$

If f^* minimizes the $J(f)$, it must be a stationary point of J . That is, $J(f + \epsilon\phi) = J(f)$, for any $\phi \in \mathcal{F}$ as $\epsilon \rightarrow 0$. More precisely, it is necessary for f^* to satisfy,

$$\forall \phi \in \mathcal{F}; \left(\frac{d}{d\epsilon} J(f^* + \epsilon\phi) \right)_{\epsilon=0} = 0. \quad (62)$$

We first construct $J(f^* + \epsilon\phi)$,

$$J(f^* + \epsilon\phi) = \frac{1}{K} \sum_k \left(\int_{\mathcal{X}} [f^* + \epsilon\phi](\mathbf{x}) \delta(\mathbf{x} - \mathbf{x}_k) d\mathbf{x} - y_k \right)^2 \quad (63)$$

$$+ c \int_{\mathcal{X}} \int_{\mathcal{X}} u(\mathbf{x}, \mathbf{x}^\dagger) [f^* + \epsilon\phi](\mathbf{x}) [f^* + \epsilon\phi](\mathbf{x}^\dagger) d\mathbf{x} d\mathbf{x}^\dagger, \quad (64)$$

or equivalently,

$$J(f^* + \epsilon\phi) = \frac{1}{K} \sum_k \left(\int_{\mathcal{X}} (f^*(\mathbf{x}) + \epsilon\phi(\mathbf{x})) \delta(\mathbf{x} - \mathbf{x}_k) d\mathbf{x} - y_k \right)^2 \quad (65)$$

$$+ c \int_{\mathcal{X}} \int_{\mathcal{X}} u(\mathbf{x}, \mathbf{x}^\dagger) (f^*(\mathbf{x}) + \epsilon\phi(\mathbf{x})) (f^*(\mathbf{x}^\dagger) + \epsilon\phi(\mathbf{x}^\dagger)) d\mathbf{x} d\mathbf{x}^\dagger. \quad (66)$$

Thus,

$$\frac{d}{d\epsilon} J(f^* + \epsilon\phi) = \frac{1}{K} \sum_k 2 \left(\int_{\mathcal{X}} (f^*(\mathbf{x}^\diamond) + \epsilon\phi(\mathbf{x}^\diamond)) \delta(\mathbf{x}^\diamond - \mathbf{x}_k) d\mathbf{x}^\diamond - y_k \right) \left(\int_{\mathcal{X}} \phi(\mathbf{x}) \delta(\mathbf{x} - \mathbf{x}_k) d\mathbf{x} \right) \quad (67)$$

$$+ c \int_{\mathcal{X}} \int_{\mathcal{X}} u(\mathbf{x}, \mathbf{x}^\dagger) \left(\phi(\mathbf{x}) (f^*(\mathbf{x}^\dagger) + \epsilon\phi(\mathbf{x}^\dagger)) + \phi(\mathbf{x}^\dagger) (f^*(\mathbf{x}) + \epsilon\phi(\mathbf{x})) \right) d\mathbf{x} d\mathbf{x}^\dagger \quad (68)$$

Setting $\epsilon = 0$,

$$\left(\frac{d}{d\epsilon} J(f^* + \epsilon\phi) \right)_{\epsilon=0} = \frac{1}{K} \sum_k 2 \left(\int_{\mathcal{X}} f^*(\mathbf{x}^\diamond) \delta(\mathbf{x}^\diamond - \mathbf{x}_k) d\mathbf{x}^\diamond - y_k \right) \left(\int_{\mathcal{X}} \phi(\mathbf{x}) \delta(\mathbf{x} - \mathbf{x}_k) d\mathbf{x} \right) \quad (69)$$

$$+ c \int_{\mathcal{X}} \int_{\mathcal{X}} u(\mathbf{x}, \mathbf{x}^\dagger) \left(\phi(\mathbf{x}) f^*(\mathbf{x}^\dagger) + \phi(\mathbf{x}^\dagger) f^*(\mathbf{x}) \right) d\mathbf{x} d\mathbf{x}^\dagger. \quad (70)$$

By the symmetry of u ,

$$\left(\frac{d}{d\epsilon} J(f^* + \epsilon\phi) \right)_{\epsilon=0} = \frac{1}{K} \sum_k 2 \left(\int_{\mathcal{X}} f^*(\mathbf{x}^\diamond) \delta(\mathbf{x}^\diamond - \mathbf{x}_k) d\mathbf{x}^\diamond - y_k \right) \left(\int_{\mathcal{X}} \phi(\mathbf{x}) \delta(\mathbf{x} - \mathbf{x}_k) d\mathbf{x} \right) \quad (71)$$

$$+ 2c \int_{\mathcal{X}} \int_{\mathcal{X}} u(\mathbf{x}, \mathbf{x}^\dagger) \phi(\mathbf{x}) f^*(\mathbf{x}^\dagger) d\mathbf{x} d\mathbf{x}^\dagger. \quad (72)$$

Factoring out ϕ ,

$$\left(\frac{d}{d\epsilon}J(f^* + \epsilon\phi)\right)_{\epsilon=0} = \int_{\mathcal{X}} 2\phi(\mathbf{x}) \left(\frac{1}{K} \sum_k \delta(\mathbf{x} - \mathbf{x}_k) \left(\int_{\mathcal{X}} f^*(\mathbf{x}^\diamond) \delta(\mathbf{x}^\diamond - \mathbf{x}_k) d\mathbf{x}^\diamond - y_k \right) \right. \quad (73)$$

$$\left. + c \int_{\mathcal{X}} u(\mathbf{x}, \mathbf{x}^\dagger) f^*(\mathbf{x}^\dagger) d\mathbf{x}^\dagger \right) d\mathbf{x}. \quad (74)$$

In order for the above to be zero for $\forall \phi \in \mathcal{F}$, it is necessary that,

$$\frac{1}{K} \sum_k \delta(\mathbf{x} - \mathbf{x}_k) \left(\int_{\mathcal{X}} f^*(\mathbf{x}^\diamond) \delta(\mathbf{x}^\diamond - \mathbf{x}_k) d\mathbf{x}^\diamond - y_k \right) + c \int_{\mathcal{X}} u(\mathbf{x}, \mathbf{x}^\dagger) f^*(\mathbf{x}^\dagger) d\mathbf{x}^\dagger = 0, \quad (75)$$

which further simplifies to,

$$\frac{1}{K} \sum_k \delta(\mathbf{x} - \mathbf{x}_k) (f^*(\mathbf{x}_k) - y_k) + c \int_{\mathcal{X}} u(\mathbf{x}, \mathbf{x}^\dagger) f^*(\mathbf{x}^\dagger) d\mathbf{x}^\dagger = 0. \quad (76)$$

We can equivalently express (76) by the following system of equations,

$$\begin{cases} \frac{1}{K} \sum_k \delta(\mathbf{x} - \mathbf{x}_k) r_k + c \int_{\mathcal{X}} u(\mathbf{x}, \mathbf{x}^\dagger) f^*(\mathbf{x}^\dagger) d\mathbf{x}^\dagger = 0 \\ r_1 = f^*(\mathbf{x}_1) - y_1 \\ \vdots \\ r_K = f^*(\mathbf{x}_K) - y_K \end{cases}. \quad (77)$$

We first focus on solving the first equation in f^* ,

$$\frac{1}{K} \sum_k \delta(\mathbf{x} - \mathbf{x}_k) r_k + c \int_{\mathcal{X}} u(\mathbf{x}, \mathbf{x}^\dagger) f^*(\mathbf{x}^\dagger) d\mathbf{x}^\dagger = 0; \quad (78)$$

later we can replace the resulted f^* in other equations to obtain r_k 's. Let $g(\mathbf{x}, \mathbf{t})$ be a function such that,

$$\int_{\mathcal{X}} u(\mathbf{x}, \mathbf{x}^\dagger) g(\mathbf{x}^\dagger, \mathbf{t}) d\mathbf{x}^\dagger = \delta(\mathbf{x} - \mathbf{t}). \quad (79)$$

Such g is called the **Green's function** of the linear operator L satisfying $[Lf](\mathbf{x}) = \int_{\mathcal{X}} u(\mathbf{x}, \mathbf{x}^\dagger) f(\mathbf{x}^\dagger) d\mathbf{x}^\dagger$. If we multiply both sides of (79) by $\frac{1}{K} \sum_k \delta(\mathbf{t} - \mathbf{x}_k) r_k$ and then integrate w.r.t. \mathbf{t} , we obtain,

$$\int_{\mathcal{X}} \left(\frac{1}{K} \sum_k r_k \delta(\mathbf{t} - \mathbf{x}_k) \int_{\mathcal{X}} u(\mathbf{x}, \mathbf{x}^\dagger) g(\mathbf{x}^\dagger, \mathbf{t}) d\mathbf{x}^\dagger \right) d\mathbf{t} \quad (80)$$

$$= \int_{\mathcal{X}} \left(\frac{1}{K} \sum_k r_k \delta(\mathbf{t} - \mathbf{x}_k) \delta(\mathbf{x} - \mathbf{t}) \right) d\mathbf{t}. \quad (81)$$

Rearranging the left hand side leads to,

$$\int_{\mathcal{X}} u(\mathbf{x}, \mathbf{x}^\dagger) \left(\frac{1}{K} \sum_k \int_{\mathcal{X}} r_k \delta(\mathbf{t} - \mathbf{x}_k) g(\mathbf{x}^\dagger, \mathbf{t}) d\mathbf{t} \right) d\mathbf{x}^\dagger \quad (82)$$

$$= \int_{\mathcal{X}} \left(\frac{1}{K} \sum_k r_k \delta(\mathbf{t} - \mathbf{x}_k) \delta(\mathbf{x} - \mathbf{t}) \right) d\mathbf{t}. \quad (83)$$

Using the sifting property of the delta function this simplifies to,

$$\int_{\mathcal{X}} u(\mathbf{x}, \mathbf{x}^\dagger) \left(\frac{1}{K} \sum_k r_k g(\mathbf{x}^\dagger, \mathbf{x}_k) \right) d\mathbf{x}^\dagger = \frac{1}{K} \sum_k r_k \delta(\mathbf{x} - \mathbf{x}_k). \quad (84)$$

We can now use the above identity to eliminate $\frac{1}{K} \sum_k r_k \delta(\mathbf{x} - \mathbf{x}_k)$ in (78) and thus obtain,

$$\int_{\mathcal{X}} u(\mathbf{x}, \mathbf{x}^\dagger) \left(\frac{1}{K} \sum_k r_k g(\mathbf{x}^\dagger, \mathbf{x}_k) \right) d\mathbf{x}^\dagger + c \int_{\mathcal{X}} u(\mathbf{x}, \mathbf{x}^\dagger) f^*(\mathbf{x}^\dagger) d\mathbf{x}^\dagger = 0, \quad (85)$$

or equivalently

$$\int_{\mathcal{X}} u(\mathbf{x}, \mathbf{x}^\dagger) \left(\frac{1}{K} \sum_k r_k g(\mathbf{x}^\dagger, \mathbf{x}_k) + c f^*(\mathbf{x}^\dagger) \right) d\mathbf{x}^\dagger = 0. \quad (86)$$

A sufficient (and also necessary, as u is assumed to have empty null space) for the above to hold is that,

$$f^*(\mathbf{x}) = -\frac{1}{cK} \sum_k r_k g(\mathbf{x}, \mathbf{x}_k). \quad (87)$$

We can now eliminate f^* in the system of equations (77) and obtain a system that only depends on r_k 's,

$$\begin{cases} r_1 = -\frac{1}{cK} \sum_k r_k g(\mathbf{x}_1, \mathbf{x}_k) - y_1 \\ \vdots \\ r_K = -\frac{1}{cK} \sum_k r_k g(\mathbf{x}_K, \mathbf{x}_k) - y_K \end{cases}. \quad (88)$$

This is a linear system in r_k and can be expressed in vector/matrix form,

$$(c\mathbf{I} + \mathbf{G})\mathbf{r} = -c\mathbf{y}. \quad (89)$$

Thus,

$$\mathbf{r} = -c(c\mathbf{I} + \mathbf{G})^{-1}\mathbf{y}, \quad (90)$$

and finally using the definition of f^* in (87) we obtain,

$$f^*(\mathbf{x}) = -\frac{1}{c} \mathbf{g}_x^T \mathbf{r} = \mathbf{g}_x^T (c\mathbf{I} + \mathbf{G})^{-1} \mathbf{y}. \quad (91)$$

B Proofs

Proposition 1 *The variational problem (13) has a solution of the form,*

$$f^*(\mathbf{x}) = \mathbf{g}_{\mathbf{x}}^T (c\mathbf{I} + \mathbf{G})^{-1} \mathbf{y}. \quad (92)$$

See Appendix A for a proof.

Proposition 2 *The following identity holds,*

$$\frac{1}{K} \sum_k (f^*(\mathbf{x}_k) - y_k)^2 = \frac{1}{K} \sum_k \left(z_k \frac{c}{c + d_k} \right)^2. \quad (93)$$

Proof

$$\frac{1}{K} (f^*(\mathbf{x}_k) - y_k)^2 \quad (94)$$

$$= \frac{1}{K} (\mathbf{g}_{\mathbf{x}_k}^T (c\mathbf{I} + \mathbf{G})^{-1} \mathbf{y} - y_k)^2 \quad (95)$$

$$= \frac{1}{K} \|\mathbf{G}(c\mathbf{I} + \mathbf{G})^{-1} \mathbf{y} - \mathbf{y}\|^2 \quad (96)$$

$$= \frac{1}{K} \|\mathbf{V}^T \mathbf{D}(c\mathbf{I} + \mathbf{D})^{-1} \mathbf{V} \mathbf{y} - \mathbf{y}\|^2, \quad (97)$$

which after exploiting rotation invariance property of $\|\cdot\|$ and the fact that the matrix of eigenvectors \mathbf{V} is a rotation matrix, can be expressed as,

$$\frac{1}{K} (f^*(\mathbf{x}_k) - y_k)^2 \quad (98)$$

$$= \frac{1}{K} \|\mathbf{V}^T \mathbf{D}(c\mathbf{I} + \mathbf{D})^{-1} \mathbf{V} \mathbf{y} - \mathbf{y}\|^2 \quad (99)$$

$$= \frac{1}{K} \|\mathbf{V} \mathbf{V}^T \mathbf{D}(c\mathbf{I} + \mathbf{D})^{-1} \mathbf{V} \mathbf{y} - \mathbf{V} \mathbf{y}\|^2 \quad (100)$$

$$= \frac{1}{K} \|\mathbf{D}(c\mathbf{I} + \mathbf{D})^{-1} \mathbf{z} - \mathbf{z}\|^2 \quad (101)$$

$$= \frac{1}{K} \left\| (\mathbf{D}(c\mathbf{I} + \mathbf{D})^{-1} - \mathbf{I}) \mathbf{z} \right\|^2 \quad (102)$$

$$= \frac{1}{K} \sum_k \left(\frac{d_k}{c + d_k} - 1 \right)^2 z_k^2 \quad (103)$$

$$= \frac{1}{K} \sum_k \left(z_k \frac{c}{c + d_k} \right)^2, \quad (104)$$

□

Proposition 3 *For any $t \geq 0$, if $\|\mathbf{z}_i\| > \sqrt{K} \epsilon$ for $i = 0, \dots, t$, then,*

$$\|\mathbf{z}_t\| \geq a^t(\kappa) \|\mathbf{z}_0\| - \sqrt{K} \epsilon b(\kappa) \frac{a^t(\kappa) - 1}{a(\kappa) - 1}, \quad (105)$$

where,

$$a(x) \triangleq \frac{(r_0 - 1)^2 + x(2r_0 - 1)}{(r_0 - 1 + x)^2} \quad (106)$$

$$b(x) \triangleq \frac{r_0^2 x}{(r_0 - 1 + x)^2} \quad (107)$$

$$r_0 \triangleq \frac{1}{\sqrt{K} \epsilon} \|\mathbf{z}_0\|, \quad \kappa \triangleq \frac{d_{\max}}{d_{\min}}. \quad (108)$$

Proof We start from the identity we obtained in (37). By diving both sides of it by $\sqrt{K}\epsilon$ we obtain,

$$\frac{1}{\sqrt{K}\epsilon} \mathbf{z}_t = \mathbf{D} \left(\frac{\alpha_t \sqrt{K}\epsilon}{\|\mathbf{z}_{t-1}\| - \sqrt{K}\epsilon} \mathbf{I} + \mathbf{D} \right)^{-1} \frac{1}{\sqrt{K}\epsilon} \mathbf{z}_{t-1}, \quad (109)$$

where,

$$d_{\min} \leq \alpha_t \leq d_{\max}. \quad (110)$$

Note that the matrix $\mathbf{D} \left(\frac{\alpha_t \sqrt{K}\epsilon}{\|\mathbf{z}_{t-1}\| - \sqrt{K}\epsilon} \mathbf{I} + \mathbf{D} \right)^{-1}$ in the above identity is *diagonal* and its k 'th entry can be expressed as,

$$\left(\mathbf{D} \left(\frac{\alpha_t \sqrt{K}\epsilon}{\|\mathbf{z}_{t-1}\| - \sqrt{K}\epsilon} \mathbf{I} + \mathbf{D} \right)^{-1} \right) [k, k] = \frac{d_k}{\frac{\alpha_t \sqrt{K}\epsilon}{\|\mathbf{z}_{t-1}\| - \sqrt{K}\epsilon} + d_k} = \frac{1}{\frac{\frac{\alpha_t}{d_k}}{\frac{\|\mathbf{z}_{t-1}\|}{\sqrt{K}\epsilon} - 1} + 1}. \quad (111)$$

Thus, as long as $\|\mathbf{z}_{t-1}\| > \sqrt{K}\epsilon$ we can get the following upper and lower bounds,

$$\frac{1}{\frac{\frac{d_{\max}}{d_{\min}}}{\frac{\|\mathbf{z}_{t-1}\|}{\sqrt{K}\epsilon} - 1} + 1} \leq \left(\mathbf{D} \left(\frac{\alpha_t \sqrt{K}\epsilon}{\|\mathbf{z}_{t-1}\| - \sqrt{K}\epsilon} \mathbf{I} + \mathbf{D} \right)^{-1} \right) [k, k] \leq \frac{1}{\frac{\frac{d_{\min}}{d_{\max}}}{\frac{\|\mathbf{z}_{t-1}\|}{\sqrt{K}\epsilon} - 1} + 1}. \quad (112)$$

Putting the above fact beside recurrence relation of \mathbf{z}_t in (109), we can bound $\frac{1}{\sqrt{K}\epsilon} \|\mathbf{z}_t\|$ as,

$$\frac{1}{\frac{\kappa}{r_{t-1}-1} + 1} r_{t-1} \leq r_t \leq \frac{1}{\frac{\frac{1}{\kappa}}{r_{t-1}-1} + 1} r_{t-1}, \quad (113)$$

where we used short hand notation,

$$\kappa \triangleq \frac{d_{\max}}{d_{\min}} \quad (114)$$

$$r_t \triangleq \frac{1}{\sqrt{K}\epsilon} \|\mathbf{z}_t\|. \quad (115)$$

Note that κ is the *condition number* of the matrix \mathbf{G} and by definition satisfies $\kappa \geq 1$. To further simplify the bounds, we use the inequality⁹,

$$\frac{1}{\frac{\frac{1}{\kappa}}{r_{t-1}-1} + 1} r_{t-1} \leq r_{t-1} \frac{(r_0 - 1)^2 + \frac{1}{\kappa}(2r_0 - 1)}{(r_0 - 1 + \frac{1}{\kappa})^2} - \frac{r_0^2 \frac{1}{\kappa}}{(r_0 - 1 + \frac{1}{\kappa})^2}, \quad (116)$$

and¹⁰,

$$\frac{1}{\frac{\kappa}{r_{t-1}-1} + 1} r_{t-1} \geq r_{t-1} \frac{(r_0 - 1)^2 + \kappa(2r_0 - 1)}{(r_0 - 1 + \kappa)^2} - \frac{r_0^2 \kappa}{(r_0 - 1 + \kappa)^2}. \quad (117)$$

⁹This follows from concavity of $\frac{x}{\frac{1}{\kappa} - x + 1}$ in x as long as $x - 1 \geq 0$ (can be verified by observing that the second derivative of the function is negative when $x - 1 \geq 0$ because $\kappa > 1$ by definition). For any function $f(x)$ that is concave on the interval $[\underline{x}, \bar{x}]$, any line tangent to f forms an *upper* bound on $f(x)$ over $[\underline{x}, \bar{x}]$. In particular, we use the tangent at the end point \bar{x} to construct our bound. In our setting, this point which happens to be r_0 . The latter is because r_t is a decreasing sequence (see beginning of Section 3.2) and thus its largest values is at $t = 0$.

¹⁰Similar to the earlier footnote, this follows from convexity of $\frac{x}{\frac{\kappa}{x-1} + 1}$ in x as long as $x - 1 \geq 0$ since $\kappa > 1$ by definition. For any function $f(x)$ that is convex on the interval $[\underline{x}, \bar{x}]$, any line tangent to f forms an *lower* bound on $f(x)$ over $[\underline{x}, \bar{x}]$. In particular, we use the tangent at the end point \bar{x} to construct our bound, which as the earlier footnote, translate into r_0 .

For brevity, we introduce,

$$a(x) \triangleq \frac{(r_0 - 1)^2 + x(2r_0 - 1)}{(r_0 - 1 + x)^2} \quad (118)$$

$$b(x) \triangleq \frac{r_0^2 x}{(r_0 - 1 + x)^2}. \quad (119)$$

Therefore, the bounds can be expressed more concisely as,

$$a(\kappa) r_{t-1} - b(\kappa) \leq r_t \leq a\left(\frac{1}{\kappa}\right) r_{t-1} - b\left(\frac{1}{\kappa}\right). \quad (120)$$

Now since both $r_{t-1} \triangleq \frac{1}{\sqrt{K}\epsilon} \|\mathbf{z}_{t-1}\|$ and $a(\kappa)$ or $a\left(\frac{1}{\kappa}\right)$ are non-negative, we can solve the recurrence¹¹ and obtain,

$$a^t(\kappa) r_0 - b(\kappa) \frac{a^t(\kappa) - 1}{a(\kappa) - 1} \leq r_t \leq a^t\left(\frac{1}{\kappa}\right) r_0 - b\left(\frac{1}{\kappa}\right) \frac{a^t\left(\frac{1}{\kappa}\right) - 1}{a\left(\frac{1}{\kappa}\right) - 1}. \quad (121)$$

□

Proposition 4 Starting from $\|\mathbf{y}_0\| > \sqrt{K}\epsilon$, meaningful (non-collapsing solution) self-distillation is possible at least for \underline{t} rounds,

$$\underline{t} \triangleq \frac{\frac{\|\mathbf{y}_0\|}{\sqrt{K}\epsilon} - 1}{\kappa}. \quad (122)$$

Proof Recall that the assumption $\|\mathbf{z}_t\| > \sqrt{K}\epsilon$ translates into $r_t > 1$. We now obtain a sufficient condition for $r_t > 1$ by requiring a lower bound on r_t to be greater than one. For that purpose, we utilize the lower bound we established in (121),

$$\underline{r}_t \triangleq a^t(\kappa) r_0 - b(\kappa) \frac{a^t(\kappa) - 1}{a(\kappa) - 1}. \quad (123)$$

Setting the above to value 1 implies,

$$\underline{r}_t = 1 \Rightarrow t = \frac{\log\left(\frac{1 - a(\kappa) + b(\kappa)}{b(\kappa) + r_0(1 - a(\kappa))}\right)}{\log(a(\kappa))} = \frac{\log\left(\frac{1 + \frac{\kappa-1}{r_0^2}}{1 + \frac{\kappa-1}{r_0}}\right)}{\log\left(1 - \frac{(\frac{\kappa-1}{r_0} + \frac{1}{r_0})(\frac{\kappa-1}{r_0})}{(1 + \frac{\kappa-1}{r_0})^2}\right)}. \quad (124)$$

Observe that,

$$\frac{\log\left(\frac{1 + \frac{\kappa-1}{r_0^2}}{1 + \frac{\kappa-1}{r_0}}\right)}{\log\left(1 - \frac{(\frac{\kappa-1}{r_0} + \frac{1}{r_0})(\frac{\kappa-1}{r_0})}{(1 + \frac{\kappa-1}{r_0})^2}\right)} \geq \frac{r_0 - 1}{\kappa}, \quad (125)$$

Thus,

$$t \geq \frac{r_0 - 1}{\kappa} = \frac{\frac{\|\mathbf{z}_0\|}{\sqrt{K}\epsilon} - 1}{\kappa} = \frac{\frac{\|\mathbf{z}_0\|}{\sqrt{K}\epsilon} - 1}{\kappa} = \frac{\frac{\|\mathbf{y}_0\|}{\sqrt{K}\epsilon} - 1}{\kappa}. \quad (126)$$

□

¹¹More compactly, the problem can be stated as $\alpha^\dagger r_{t-1} - b \leq r_t \leq \alpha r_{t-1} - b$, where $\alpha > 0$ and $\alpha^\dagger > 0$. Let's focus on $r_t \leq \alpha r_{t-1} - b$, as the other case follows by similar argument. Start from the base case $r_1 \leq \alpha r_0 - b$. Since $\alpha > 0$, we can multiply both sides by that and then add $-b$ to both sides: $\alpha r_1 - b \leq \alpha^2 r_0 - b(\alpha + 1)$. On the other hand, looking at the recurrence $r_t \leq \alpha r_{t-1} - b$ at $t = 2$ yields $r_2 \leq \alpha r_1 - b$. Combining the two inequalities gives $r_2 \leq \alpha^2 r_0 - b(\alpha + 1)$. By repeating this argument we obtain the general case $r_t \leq \alpha^t r_0 - b(\sum_{j=0}^{t-1} \alpha^j)$.

Proposition 5 Suppose $\|\mathbf{y}_0\| > \sqrt{K}\epsilon$ and $t \leq \frac{\|\mathbf{y}_0\|}{\kappa\sqrt{K}\epsilon} - \frac{1}{\kappa}$. Then for any pair of diagonals of \mathbf{D} , namely d_j and d_k , with the condition that $d_k > d_j$, the following inequality holds.

$$\frac{\mathbf{B}_{t-1}[k, k]}{\mathbf{B}_{t-1}[j, j]} \geq \left(\frac{\frac{\|\mathbf{y}_0\|}{\sqrt{K}\epsilon} - 1 + \frac{d_{\min}}{d_j}}{\frac{\|\mathbf{y}_0\|}{\sqrt{K}\epsilon} - 1 + \frac{d_{\min}}{d_k}} \right)^t. \quad (127)$$

Proof We start with the definition of \mathbf{A}_t from (30) and proceed as,

$$\frac{\mathbf{A}_t[k, k]}{\mathbf{A}_t[j, j]} = \frac{1 + \frac{c_t}{d_j}}{1 + \frac{c_t}{d_k}}. \quad (128)$$

Since the derivative of the r.h.s. above w.r.t. c_t is non-negative as long as $d_k \geq d_j$, it is non-decreasing in c_t . Therefore, we can get a lower bound on r.h.s. using a lower bound on c_t (denoted by \underline{c}_t),

$$\frac{\mathbf{A}_t[k, k]}{\mathbf{A}_t[j, j]} \geq \frac{1 + \frac{\underline{c}_t}{d_j}}{1 + \frac{\underline{c}_t}{d_k}}. \quad (129)$$

Also, since the assumption $t \leq \frac{\|\mathbf{y}_0\|}{\kappa\sqrt{K}\epsilon} - \frac{1}{\kappa}$ guarantees non-collapse conditions $c_t > 0$ and $\|\mathbf{z}_t\| > \sqrt{K}\epsilon$, we can apply (36) and have the following lower bound on c_t

$$c_t \geq \frac{d_{\min}\sqrt{K}\epsilon}{\|\mathbf{z}_t\| - \sqrt{K}\epsilon}. \quad (130)$$

Since the r.h.s. (130) is decreasing in $\|\mathbf{z}_t\|$, the smallest value for the r.h.s. is attained by the largest value of $\|\mathbf{z}_t\|$. However, as $\|\mathbf{z}_t\|$ is decreasing in t (see beginning of Section 3.2), its largest value is attained at $t = 0$. Putting these together we obtain,

$$c_t \geq \frac{d_{\min}\sqrt{K}\epsilon}{\|\mathbf{z}_0\| - \sqrt{K}\epsilon}. \quad (131)$$

Using the r.h.s. of the above as \underline{c}_t and applying it to (129) yields,

$$\frac{\mathbf{A}_t[k, k]}{\mathbf{A}_t[j, j]} \geq \frac{\frac{\|\mathbf{z}_0\|}{\sqrt{K}\epsilon} - 1 + \frac{d_{\min}}{d_j}}{\frac{\|\mathbf{z}_0\|}{\sqrt{K}\epsilon} - 1 + \frac{d_{\min}}{d_k}}. \quad (132)$$

Notice that both sides of the inequality are positive; \mathbf{A}_t based on its definition in (30) and r.h.s. by the fact that $\|\mathbf{z}_0\| \geq \sqrt{K}\epsilon$. Therefore, we can instantiate the above inequality at each distillation step i , for $i = 0, \dots, t-1$, and multiply them to obtain,

$$\prod_{i=0}^{t-1} \frac{\mathbf{A}_i[k, k]}{\mathbf{A}_i[j, j]} \geq \left(\frac{\frac{\|\mathbf{z}_0\|}{\sqrt{K}\epsilon} - 1 + \frac{d_{\min}}{d_j}}{\frac{\|\mathbf{z}_0\|}{\sqrt{K}\epsilon} - 1 + \frac{d_{\min}}{d_k}} \right)^t. \quad (133)$$

or equivalently,

$$\frac{\mathbf{B}_{t-1}[k, k]}{\mathbf{B}_{t-1}[j, j]} \geq \left(\frac{\frac{\|\mathbf{z}_0\|}{\sqrt{K}\epsilon} - 1 + \frac{d_{\min}}{d_j}}{\frac{\|\mathbf{z}_0\|}{\sqrt{K}\epsilon} - 1 + \frac{d_{\min}}{d_k}} \right)^t. \quad (134)$$

□

Proposition 6 Suppose $\|\mathbf{y}_0\| > \sqrt{K}\epsilon$. Then the sparsity index $S_{\mathbf{B}_{\underline{t}-1}}$ (where $\underline{t} = \frac{\|\mathbf{y}_0\|}{\kappa\sqrt{K}\epsilon} - \frac{1}{\kappa}$ is number of guaranteed self-distillation steps before solution collapse) “decreases” in ϵ , i.e. lower ϵ yields higher sparsity.

Furthermore at the limit $\epsilon \rightarrow 0$, the sparsity index has the form,

$$\lim_{\epsilon \rightarrow 0} S_{\mathbf{B}_{\underline{t}-1}} = e^{\frac{d_{\min}}{\kappa} \min_{k \in \{1, 2, \dots, K-1\}} \left(\frac{1}{d_k} - \frac{1}{d_{k+1}} \right)}. \quad (135)$$

Proof We first show that the sparsity index is decreasing in ϵ . We start from the definition of the sparsity index $S_{\mathbf{B}_{t-1}}$ in (51) which we repeat below,

$$S_{\mathbf{B}_{t-1}} = \min_{k \in \{1, 2, \dots, K-1\}} \left(\frac{\frac{\|\mathbf{y}_0\|}{\sqrt{K}\epsilon} - 1 + \frac{d_{\min}}{d_k}}{\frac{\|\mathbf{y}_0\|}{\sqrt{K}\epsilon} - 1 + \frac{d_{\min}}{d_{k+1}}} \right)^{\frac{\|\mathbf{y}_0\|}{\kappa\sqrt{K}\epsilon} - \frac{1}{\kappa}}. \quad (136)$$

For brevity, we define base and exponent as,

$$b \triangleq \frac{m + \frac{d_{\min}}{d_k}}{m + \frac{d_{\min}}{d_{k+1}}} \quad (137)$$

$$p \triangleq \frac{m}{\kappa} \quad (138)$$

$$m \triangleq \frac{\|\mathbf{y}_0\|}{\sqrt{K}\epsilon} - 1, \quad (139)$$

so that,

$$S_{\mathbf{B}_{t-1}}(\epsilon) = b^p. \quad (140)$$

The derivative is thus,

$$\frac{d}{d\epsilon} S_{\mathbf{B}_{t-1}} \quad (141)$$

$$= \frac{d S_{\mathbf{B}_{t-1}}}{dm} \frac{dm}{d\epsilon} \quad (142)$$

$$= \left(b^p \left(\frac{p b_m}{b} + p_m \log(b) \right) \right) \left(\frac{dm}{d\epsilon} \right) \quad (143)$$

$$= b^p \left(\frac{p b_m}{b} + p_m \log(b) \right) \left(-\frac{1}{2\epsilon} (m+1) \right) \quad (144)$$

$$= b^p \left(\frac{p}{m + \frac{d_{\min}}{d_k}} - \frac{p}{m + \frac{d_{\min}}{d_{k+1}}} + \frac{1}{\kappa} \log(b) \right) \left(-\frac{1}{2\epsilon} (m+1) \right) \quad (145)$$

$$= \frac{b^p}{\kappa} \left(\frac{m}{m + \frac{d_{\min}}{d_k}} - \frac{m}{m + \frac{d_{\min}}{d_{k+1}}} + \log(b) \right) \left(-\frac{1}{2\epsilon} (m+1) \right) \quad (146)$$

$$= \frac{b^p}{\kappa} \left(\frac{1}{1 + \frac{d_{\min}}{m d_k}} - \frac{1}{1 + \frac{d_{\min}}{m d_{k+1}}} + \log(b) \right) \left(-\frac{1}{2\epsilon} (m+1) \right) \quad (147)$$

$$= \frac{b^p}{\kappa} \left(\frac{1}{1 + \frac{d_{\min}}{m d_k}} - \frac{1}{1 + \frac{d_{\min}}{m d_{k+1}}} + \log\left(\frac{1 + \frac{d_{\min}}{m d_k}}{1 + \frac{d_{\min}}{m d_{k+1}}}\right) \right) \left(-\frac{1}{2\epsilon} (m+1) \right) \quad (148)$$

$$= \frac{b^p}{\kappa} \left(\frac{1}{1 + \frac{d_{\min}}{m d_k}} + \log\left(1 + \frac{d_{\min}}{m d_k}\right) - \frac{1}{1 + \frac{d_{\min}}{m d_{k+1}}} - \log\left(1 + \frac{d_{\min}}{m d_{k+1}}\right) \right) \left(-\frac{1}{2\epsilon} (m+1) \right). \quad (149)$$

We now focus on the first parentheses. Define the function $e(x) \triangleq \frac{1}{x} + \log(x)$. Thus we can write the contents in the first parentheses more compactly,

$$\frac{1}{1 + \frac{d_{\min}}{m d_k}} + \log\left(1 + \frac{d_{\min}}{m d_k}\right) - \frac{1}{1 + \frac{d_{\min}}{m d_{k+1}}} - \log\left(1 + \frac{d_{\min}}{m d_{k+1}}\right) \quad (150)$$

$$= e\left(1 + \frac{d_{\min}}{m d_k}\right) - e\left(1 + \frac{d_{\min}}{m d_{k+1}}\right). \quad (151)$$

However, $e'(x) = \frac{x-1}{x^2}$, thus when $x > 1$ the function $e'(x)$ is positive. Consequently, when $x > 1$ $e(x)$ is increasing. In fact, since both $\frac{d_{\min}}{m d_k}$ and $\frac{d_{\min}}{m d_{k+1}}$ are positive, the arguments of e satisfy the

condition of being greater than 1 and thus e is increasing. On the other hand, since $d_{k+1} > d_k$ it follows that $1 + \frac{d_{\min}}{m d_k} > 1 + \frac{d_{\min}}{m d_{k+1}}$, and thus by leveraging the fact that e is increasing we obtain $e(1 + \frac{d_{\min}}{m d_k}) > e(1 + \frac{d_{\min}}{m d_{k+1}})$. Finally by plugging the definition of e we obtain,

$$\frac{1}{1 + \frac{d_{\min}}{m d_k}} + \log(1 + \frac{d_{\min}}{m d_k}) > \frac{1}{1 + \frac{d_{\min}}{m d_{k+1}}} + \log(1 + \frac{d_{\min}}{m d_{k+1}}). \quad (152)$$

It is now easy to determine the sign of $\frac{d}{d\epsilon} S$ as shown below,

$$\begin{aligned} & \frac{d}{d\epsilon} S_{\mathcal{B}_{\ell-1}} \quad (153) \\ = & \underbrace{\frac{b^p}{\kappa}}_{\text{positive}} \left(\underbrace{\frac{1}{1 + \frac{d_{\min}}{m d_k}} + \log(1 + \frac{d_{\min}}{m d_k}) - \frac{1}{1 + \frac{d_{\min}}{m d_{k+1}}} - \log(1 + \frac{d_{\min}}{m d_{k+1}})}_{\text{positive}} \right) \underbrace{\left(-\frac{1}{2\epsilon}(m+1) \right)}_{\text{negative}} \quad (154) \end{aligned}$$

By showing that $\frac{d}{d\epsilon} S_{\mathcal{B}_{\ell-1}} < 0$ we just proved $S_{\mathcal{B}_{\ell-1}}$ is decreasing in ϵ .

We now focus on the limit case $\epsilon \rightarrow 0$. First note due to the identity $m = \frac{\|\mathbf{y}_0\|}{\sqrt{K}\epsilon} - 1$ we have the following identity,

$$\lim_{\epsilon \rightarrow 0} \min_{k \in \{1, 2, \dots, K-1\}} \left(\frac{\frac{\|\mathbf{y}_0\|}{\sqrt{K}\epsilon} - 1 + \frac{d_{\min}}{d_k}}{\frac{\|\mathbf{y}_0\|}{\sqrt{K}\epsilon} - 1 + \frac{d_{\min}}{d_{k+1}}} \right)^{\frac{\|\mathbf{y}_0\|}{\sqrt{K}\epsilon} - \frac{1}{\kappa}} \quad (155)$$

$$= \lim_{m \rightarrow \infty} \min_{k \in \{1, 2, \dots, K-1\}} \left(\frac{m + \frac{d_{\min}}{d_k}}{m + \frac{d_{\min}}{d_{k+1}}} \right)^{\frac{1}{\kappa} m}. \quad (156)$$

Further, since pointwise minimum of continuous functions is also a continuous function, we can move the limit inside the minimum,

$$\lim_{m \rightarrow \infty} \min_{k \in \{1, 2, \dots, K-1\}} \left(\frac{m + \frac{d_{\min}}{d_k}}{m + \frac{d_{\min}}{d_{k+1}}} \right)^{\frac{1}{\kappa} m} \quad (157)$$

$$= \min_{k \in \{1, 2, \dots, K-1\}} \lim_{m \rightarrow \infty} \left(\frac{m + \frac{d_{\min}}{d_k}}{m + \frac{d_{\min}}{d_{k+1}}} \right)^{\frac{1}{\kappa} m} \quad (158)$$

$$= \min_{k \in \{1, 2, \dots, K-1\}} e^{\frac{d_{\min}}{d_k} - \frac{d_{\min}}{d_{k+1}} \frac{1}{\kappa}} \quad (159)$$

$$= \min_{k \in \{1, 2, \dots, K-1\}} e^{\frac{d_{\min}}{\kappa} \left(\frac{1}{d_k} - \frac{1}{d_{k+1}} \right)} \quad (160)$$

$$= e^{\frac{d_{\min}}{\kappa} \min_{k \in \{1, 2, \dots, K-1\}} \left(\frac{1}{d_k} - \frac{1}{d_{k+1}} \right)}, \quad (161)$$

where in (159) we used the identity $\lim_{x \rightarrow \infty} f(x)^{g(x)} = e^{\lim_{x \rightarrow \infty} (f(x)-1)(g(x))}$ and in (161) we used the fact that $e^{\frac{d_{\min}}{\kappa} x}$ is monotonically increasing in x (because $\frac{d_{\min}}{\kappa} > 0$). \square

C More on Experiments

C.1 Setup Details

We used Adam optimizer with learning rates of 0.001 and 0.0001 for CIFAR-10 and CIFAR-100, respectively. They are trained up to 64000 steps with batch size equal to 16 and 64 for CIFAR-10 and CIFAR-100, respectively. In all the experiments, we slightly regularize the training by weight decay regularization added to the fitting loss with its coefficient set to 0.0001 and 0.00005 for CIFAR-10 and CIFAR-100, respectively. Training and test is performed on the standard (50000 train-10000 test) split of the CIFAR dataset. Most of the experiments are conducted using Resnet-50 [He et al., 2015] and CIFAR-10 and CIFAR-100 datasets [Krizhevsky, 2009]. However, we briefly validate our results on VGG-16 [Simonyan and Zisserman, 2015] too.

C.2 ℓ_2 Loss on Neural Network Predictions

Figure 7 shows the full results on CIFAR-10 and Resnet-50. The train and test accuracies have already been discussed in the main paper and are copied here to facilitate comparison. However, in this subsection, we demonstrated the loss of the trained model at all steps with respect to the original ground truth data too. This may help establish an intuition on how self-distillation is regularizing the training on the original data. Looking at the train loss we can see it first drops as the regularization is amplified and then increases while the model under-fits. This, again, suggests that the mechanism that self-distillation employs for regularization is different from early stopping. For CIFAR-100 the results in Figure 8 show a similar trend.

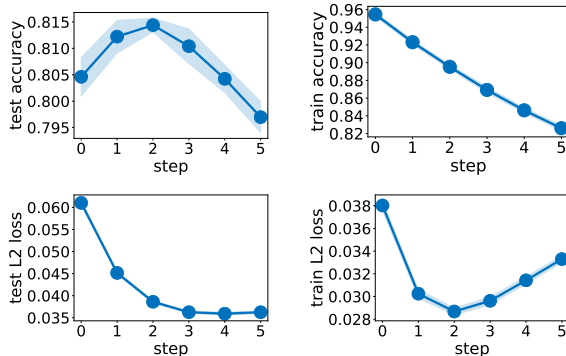


Figure 7: Self distillation results with ℓ_2 loss of neural network predictions for Resnet-50 and CIFAR-10

C.3 Self-distillation on Hard Labels

One might wonder how self-distillation would perform if we replace the neural network (soft) predictions with hard labels. In other words, the teacher’s predictions are turned into one-hot-vector via `argmax` and they are treated like a dataset with augmented labels. Of-course, since the model is already over-parameterized and trained close to interpolation regime only a small fraction of labels will change. Figures 9 and 10 show the results of self distillation using cross entropy loss on labels predicted by the teacher model. Surprisingly, self-distillation improves the performance here too. This observation may be related to learning under noisy dataset and calls for more future work on this interesting case.

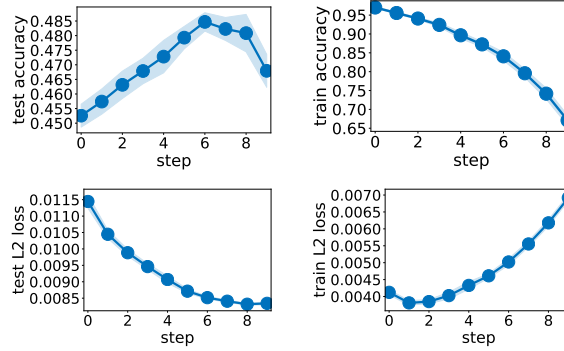


Figure 8: Self distillation results with ℓ_2 loss of neural network predictions for Resnet-50 and CIFAR-100

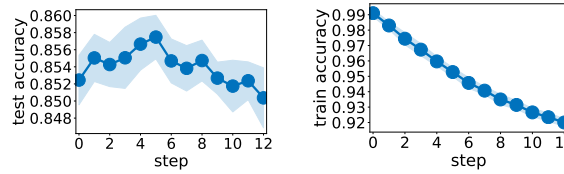


Figure 9: Self distillation results with cross entropy loss on hard labels for Resnet-50 and CIFAR-10

D Mathematica Code To Reproduce Illustrative Example

```
x = (Table[i, {i, -5, 5}]/5 + 1)/2;
y = Sin[x*2*Pi] +
  RandomVariate[NormalDistribution[0, 0.5], Length[x]]
ListPlot[y]

(* UNCOMMENT IF YOU WISH TO USE EXACT SAME RANDOM SAMPLES IN THE PAPER *)
(* y = {0.38476636465198066',
  1.2333967683416893', 1.33232242218057',
  0.6920159488889518', -0.29756145531871736', -0.24189291901377769', \
-0.79644857691756675', -0.9616480167034174', -0.49672509509916934', \
-0.3469066003991437', 0.5589512650600734'}; *)

(***** PLOT GREEN'S FUNCTION g0(X,T) FOR OPERATOR d^4/dx^4 *****)

g0 = 1/6*Max[{(T - X)^3, 0}] - 1/6*T*(1 - X)*(T^2 - 2*X + X^2);
ContourPlot[g0, {X, 0, 1}, {T, 0, 1}]
Plot3D[g0, {X, 0, 1}, {T, 0, 1}]

(***** COMPUTE g AND G *****)

G = Table[
  g0 /. X -> ((i/5 + 1)/2) /. T -> ((j/5 + 1)/2), {i, -5, 5}, {j, -5,
  5}];
g = Transpose[{Table[g0 /. T -> ((j/5 + 1)/2), {j, -5, 5}]}];

(***** PLOT GROUND-TRUTH FUNCTION (ORANGE) AND OVERFIT FUNCTION \
(BLUE) *****)
FNoReg = (Transpose[g].Inverse[
  G + 0.0000000001*IdentityMatrix[Length[x]]].Transpose[{y}])[[1,
  1]];
pts = Table[{x[[i]], y[[i]]}, {i, 1, Length[x]}];
```

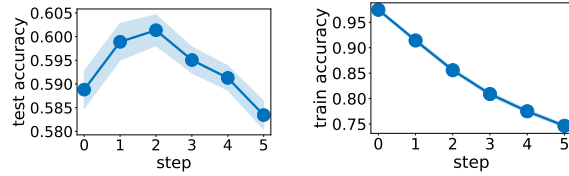


Figure 10: Self distillation results with cross entropy loss on hard labels for Resnet-50 and CIFAR-100

```
Show[{ListPlot[pts], Plot[{FNoReg, Sin[X*2*Pi]}, {X, 0, 1}]}]
```

```
(**** PARAMETERS ****)
```

```
MaxIter = 10;
eps = 0.045;
```

```
(**** SUBROUTINES ****)
```

```
Loss[G_, yin_, c_] := Module[
  {t = (G.Inverse[c*IdentityMatrix[Length[yin]] + G] -
    IdentityMatrix[Length[x]]) . yin},
  Total[Flatten[t]^2]/Length[yin]
];
```

```
FindRootsC[f_, c_] := Module[
  {Sol = Quiet[Solve[f == 0, c]], Sel},
  Sel = Select[
    c /. Sol, (Abs[Im[#]] < 0.00000001) && # > 0.00000001 &]
];
```

```
(**** MAIN ****)
```

```
(* Initialization *)
```

```
y0 = Transpose[{y}];
ycur = y0;
B = IdentityMatrix[Length[x]];
FunctionSequence = {};
ASequence = {};
BSequence = {};
```

```
(* Self-Distillation Loop *)
```

```
For[i = 1;, i < MaxIter, i++,
  Print["Iteration ", i];
  Print["Norm[y]=", Norm[ycur]];
  L = Loss[G, ycur, c];
  RootsC = FindRootsC[L - eps, c];
  Switch [Length[RootsC], 0, (Print["No Root"]; Break[;]), 1,
    Print["Found Unique Root c=", RootsC[[1]] ]];
  (* Now that root is unique *)
  RootC = RootsC[[1]];
  Print["Achieved Loss Value ", Loss[G, ycur, RootC]];
  U = G.Inverse[G + RootC*IdentityMatrix[Length[ycur]]];
  A = DiagonalMatrix[Eigenvalues[U]];
  f = (Transpose[g].Inverse[
    G + RootC*IdentityMatrix[Length[ycur]]].ycur)[[1, 1]];
  B = B.A;
  ycur = U.ycur;
```

```
FunctionSequence = Append[FunctionSequence, f];
ASequence = Append[ASequence, Diagonal[A]];
BSequence = Append[BSequence, Diagonal[B]];
```

```
]
If[i == MaxIter, Print["Max Iterations Reached!"]]

Plot[FunctionSequence, {X, 0, 1}]
BarChart[ASequence, ChartStyle -> "DarkRainbow", AspectRatio -> 0.2,
  ImageSize -> Full]
BarChart[BSequence, ChartStyle -> "DarkRainbow", AspectRatio -> 0.2,
  ImageSize -> Full]
```

E Python Implementation

Implementing self-distillation is quite straight forward provided with merely a customized loss that replaces the ground-truth labels with teacher predictions. Here, we provide a Tensorflow implementation of the self-distillation loss function:

```
1 def self_distillation_loss(labels, logits, model, reg_coef, teacher=None
  , data=None):
2     if teacher is None:
3         main_loss = tf.reduce_mean(tf.squared_difference(labels,
4                                                         tf.nn.softmax(
5                                                             logits)))
6     else:
7         main_loss = tf.reduce_mean(tf.squared_difference(tf.nn.softmax(
8                                                         teacher(data)),
9                                                         tf.nn.softmax(
10                                                            logits)))
11
12     reg_loss = reg_coef*tf.add_n([tf.nn.l2_loss(w) for w in model.
13                                 trainable_weights])
14     total_loss = main_loss + reg_loss
15     return total_loss
```

The following snippet also demonstrates how one can use the above loss function to train a neural network using self-distillation.

```
1 def self_distillation_train(model, train_dataset, optimizer, reg_coef=1e
  -4,
2                             epochs=30, teacher=None):
3     for epoch in range(epochs):
4         for iter, (x_batch_train, y_batch_train) in enumerate(train_dataset)
5             :
6             with tf.GradientTape() as tape:
7                 logits = model(x_batch_train, training=True)
8                 loss_value = self_distillation_loss(y_batch_train, logits, model
9                                                     ,
10                                                     reg_coef, teacher,
11                                                     x_batch_train)
12                 grads = tape.gradient(loss_value, model.trainable_weights)
13                 optimizer.apply_gradients(zip(grads, model.trainable_weights))
14     return model
15
16 teacher = None
17 for step in range(distillation_steps):
18     model = get_resnet_model()
19     optimizer = keras.optimizers.Adam(learning_rate=learning_rate)
20     model = self_distillation_train(model, train_dataset, optimizer,
21                                   reg_coef, epochs, teacher)
22     teacher = model
```

The complete executable code is listed below.

```
1 # Copyright 2020 Self-Distillation Authors.
2
3
4 # Licensed under the Apache License, Version 2.0 (the "License");
5 # you may not use this file except in compliance with the License.
```

```

6 # You may obtain a copy of the License at
7
8 # https://www.apache.org/licenses/LICENSE-2.0
9
10 # Unless required by applicable law or agreed to in writing, software
11 # distributed under the License is distributed on an "AS IS" BASIS,
12 # WITHOUT WARRANTIES OR CONDITIONS OF ANY KIND, either express or
    implied.
13 # See the License for the specific language governing permissions and
14 # limitations under the License.
15
16 # This code has been tested on Colab using Tensorflow version 1.15.0,
17 # Keras version 2.2.5, and numpy version 1.17.5
18
19 import tensorflow as tf
20 from tensorflow import keras
21 tf.enable_eager_execution()
22
23 # the main loss function for training with self-distillation
24 def self_distillation_loss(labels, logits, model, reg_coef, teacher=None
    , data=None):
25     if teacher is None:
26         main_loss = tf.reduce_mean(tf.squared_difference(labels,
27                                                         tf.nn.softmax(
28                                                             logits)))
29     else:
30         main_loss = tf.reduce_mean(tf.squared_difference(tf.nn.softmax(
31                                                         teacher(data)),
32                                                         tf.nn.softmax(
33                                                             logits)))
34
35     reg_loss = reg_coef*tf.add_n([tf.nn.l2_loss(w) for w in model.
36                                 trainable_weights])
37     total_loss = main_loss + reg_loss
38     return total_loss
39
40 def get_metrics(model, x_test, y_test, teacher=None):
41     y_test_pred = model.predict(x_test)
42     acc = tf.reduce_mean(tf.cast(tf.nn.in_top_k(y_test_pred, tf.argmax(
43         y_test, axis=1),
44                                         k=1), tf.float32))
45     loss = self_distillation_loss(y_test, y_test_pred, model, reg_coef,
46                                 teacher, x_test)
47     return acc.numpy(), loss.numpy()
48
49 def get_cifar10():
50     (x_train, y_train), (x_test, y_test) = keras.datasets.cifar10.
51         load_data()
52     x_train, x_test = x_train.astype('float32') / 255., x_test.astype('
53         float32') / 255.
54     y_train, y_test = keras.utils.to_categorical(y_train, 10), keras.utils
55         .to_categorical(y_test, 10)
56     return x_train, y_train, x_test, y_test
57
58 def get_resnet_model():
59     return keras.applications.resnet.ResNet50(
60         include_top=True, weights=None, input_tensor=None,

```



```

51     input_shape=[32, 32, 3], classes=10)
52
53 # the main training procedure for single step of self-distillation
54 def self_distillation_train(model, train_dataset, optimizer, reg_coef=1e
    -5,
55                             epochs=60, teacher=None):
56     for epoch in range(epochs):
57         print('Start of epoch %d' % (epoch,))
58         for iter, (x_batch_train, y_batch_train) in enumerate(train_dataset)
            :
59             with tf.GradientTape() as tape:
60                 logits = model(x_batch_train, training=True)
61                 loss_value = self_distillation_loss(y_batch_train, logits, model
                    ,
62                                                     reg_coef, teacher,
                                                         x_batch_train)
63                 grads = tape.gradient(loss_value, model.trainable_weights)
64                 optimizer.apply_gradients(zip(grads, model.trainable_weights))
65             if verbose and epoch % 2 == 0:
66                 acc, loss = get_metrics(model, x_test, y_test, teacher)
67                 print('epoch %d test accuracy %s and loss %s (for 1 batch)' % (
                    epoch, acc, loss))
68     return model
69
70 # hyperparameters
71 batch_size = 16
72 epochs = 20 # ~64000*16/5000
73 reg_coef = 1e-4
74 learning_rate = 1e-3
75
76 # self-distillation parameters
77 distillation_steps = 10
78 verbose = True
79
80 # reading data
81 x_train, y_train, x_test, y_test = get_cifar10()
82 train_dataset = tf.data.Dataset.from_tensor_slices((x_train, y_train))
83 train_dataset = train_dataset.shuffle(buffer_size=1024).batch(batch_size
    )
84
85 # self-distillation steps
86 teacher = None
87 test_accs = []
88 for step in range(distillation_steps):
89     model = get_resnet_model()
90     optimizer = keras.optimizers.Adam(learning_rate=learning_rate)
91     model = self_distillation_train(model, train_dataset, optimizer,
        reg_coef, epochs, teacher)
92
93     acc, loss = get_metrics(model, x_test, y_test, teacher)
94     test_accs.append(acc)
95     print('distillation step %d, test accuracy %f and loss %f ' % (step,
        acc, loss))
96     teacher = model

```